1  Manuscript type: Research article

# 2  Assessing Landslide Damming susceptibility in Central Asia

3  Carlo Tacconi Stefanelli[a,b,*], William Frodella[a,b], Francesco Caleca[a,b], Zhanar Raimbekova[c,d],

4  Ruslan Umuraliev[e], Veronica Tofani[a,b]

5  [a] University of Florence, Department of Earth Sciences, via G. la Pira 4, 50121 Florence, Italy

6  [b] UNESCO Chair on the Prevention and Sustainable Management of Geo-Hydrological Hazards, University of

7  Florence, Largo Fermi 2, 50125 Florence, Italy

8  [c] Institute of Seismology of Republic of Kazakhstan (IS), Almaty, Kazakhstan

9  [d] Al-Farabi Kazakh National University, Department of Geography and Environmental Sciences, Al-Farabi ave.

10  71, A15E3C7 Almaty, Kazakhstan

11  [e] Institute of Seismology of the National Academy of Sciences of Kyrgyz Republic (ISNASKR), Bishkek, Kyrgyz

12  Republic

13  *       *Correspondence to*: carlo.tacconistefanelli@unifi.it

14  **Abstract**

15  Central Asia regions are characterized by active tectonics, high mountain chains with extreme topography with

16  glaciers and strong seasonal rainfall events. These key predisposing factors make large landslides a serious natural

17  threat in the area, causing several casualties every year. The mountain crests are divided by wide lenticular or

18  narrow, linear intermountain tectonic depressions, which are incised by many of the most important Central Asia

19  rivers and are also subject to major seasonal river flood hazard. This multi-hazard combination is a source of

20  potential damming scenarios which can bring cascading effects with devastating consequences for the surrounding

21  settlements and population. Different hazards can only be managed with a multi-hazard approach coherent within

22  the different countries, as suggested by the requirements of the Sendai Framework for Disaster Risk Reduction.

23  This work was carried out within the framework of the SFRARR Project ("*Strengthening Financial Resilience*

24  *and Accelerating Risk Reduction in Central Asia*") as a part of a multi-hazard approach with the aim of providing

25  a damming susceptibility analysis at a regional scale for Central Asia. To achieve this, a semi-automated GIS-

26  based mapping method, centred on a bivariate correlation of morphometric parameters defined by a morphological

27  index, originally designed to assess the damming susceptibility at basin/regional scale, was modified to be adopted

28  nationwide and applied to spatially assess the obstruction of the river network in Central Asia for mapped and

29  newly formed landslides. The proposed methodology represents an improvement of the previously designed,

30  requiring a smaller amount of data, bringing new preliminary information on the damming hazard management

31  and risk reduction identifying the most critical area within the Central Asia regions.

## 1 Introduction

The mountainous areas of the Djungaria, Tien Shan, Pamir and Kopetdag in Central Asia territories are characterized by complex and active tectonic and are the sources of most of Central Asia rivers. A rugged topography along with complex geological structure and high seismicity are ideal setting for large slope failures. In general, when landslides completely obstruct a river channel, they generate a landslide dam whose consequences can be a serious hazard forming upstream backwater and causing catastrophic downstream flooding, changes in the riverbed, embankments instability triggering other landslides with a cascading effect (Swanson et al., 1986; Costa and Schuster, 1988; Casagli and Ermini,1999). The effects of impounded water and anomalous flood waves, resulting from a dam breach, have significant economic and social impacts in upstream and downstream areas with economic and human losses (King et al., 1989; Dai et al., 2005; Chen and Chang, 2016). Rebuilding costs can be extensive, as they are direct (e.g., infrastructure and buildings reconstruction, safety measures) and indirect (e.g., loss in real estate value and damage caused to industrial and agricultural production), harder to estimate.

Most of landslide dams have a short life as about 40% of them collapse within 24 hours after formation and about 80% within one year (Costa and Schuster, 1988; Tacconi Stefanelli et al., 2015; Fan et al., 2020). Given the limited available time, a complete and reliable analysis of the risks, requiring in-depth study of the phenomenon, is not achievable during the event and only rapid assessments for the dam stability are suitable. When the people to evacuate are too many or the related risk is too high, engineering measures for the hazard reduction are attempted: among these are for example modification of slope geometry, drainage, retaining structures and internal slope reinforcement (Popescu and Sasahara, 2009; Schuster and Evans, 2011). Therefore, part of the effects from landslide damming can be avoided or at least reduced thanks to mitigation and prevention measures (e.g., slopes stabilization or re-profiling) if the most critical areas with the highest damming probability are known. Consequently, planning and prevention tools, such as risk and susceptibility mapping, are essential to reduce the costs of natural hazard and improve the efficiency of environmental management.

Reactivation of ancient landslides triggered during different climatic and environmental conditions may often generate new mass movements (Casagli and Ermini, 1999; Canuti et al., 2004; Dikau and Schrott, 1999; Borgatti and Soldati, 2010; Crozier, 2010). Landslides generated in the past are often dormant, with strength parameters of the sliding surface close to the residual ones, and difficult to recognize because vegetation, erosion and superficial alteration hide their morphology. Natural causes, such as earthquakes, river undercutting, rainfall, and snowmelt, or even anthropic activity can reactivate these ancient phenomena. Therefore, all dormant landslides capable to reach a river along their pathway can potentially dam it and should be investigated. New landslides, instead, may develop wherever are present suitable conditions along the slopes. The spatial occurrence probability is commonly assessed by landslide susceptibility analysis, highly dependent on landslide volume (Catani et al., 2016), which is difficult to accurately predict.

Landslides in Central Asia are quite common and a considerable number of them have huge dimension, often induced by strong earthquakes but also by floods, heavy rainfall and snowmelt (Behling et al., 2014; Golovko et al., 2015; Havenith et al., 2015a; 2015b; 2006b; Kalmetieva et al., 2009; Rosi et al., 2023; Saponaro et al., 2014; Strom and Abdrakhmatov, 2017; 2018). Concerning landslide dam events, in Central Asia regions several mass

movements of considerable size produced the obstruction of a river section, of which more than 100 still are existing with a lake (Strom, 2010). Although many of these could be considered stable (Strom, 2010), the occurrence of devastating outburst floods in the last century show that their potential hazard should never be overlooked also considering the seismicity of the region. In the Rushan and Murgab districts of Gorno-Badakhshan Autonomous Oblast (Pamirs, Tajikistan) along the Murghab river, the Usoi landslide dam is one of the most famous of the many cases in the regions. Its impounded lake, called Lake Sarez, is 60 km long with 500 m of depth and has a stored volume of about 17 km$^3$, representing the world deepest landslide-dammed lake (Costa and Schuster, 1991; Fan et al., 2020). It was originated on February 18th, 1911, when a MW 7.2 earthquake triggered a giant wedge-failure of about 2.2 km$^3$ of rock (mainly quartzite, schist, shale and dolomite) and debris that blocked the Murgab River and a tributary valley, forming the 560 m high, 5 km long and 4 km wide Usoi dam, impounding Lake Sarez, also creating the smaller Lake Shadau (Strom, 2010).

Landslide dam evolution, according to some studies (Swanson et al., 1986; Ermini and Casagli, 2003; Dal Sasso et al., 2014; Tacconi Stefanelli et al., 2016), can be estimated through geomorphological indexes which require parameters characterizing the landslide (or the dam) and the river (or the lake). Geomorphological indexes are a powerful classification tool, but their prediction power depend mainly on long studies, a large amount of data and measurement efforts given their empirical nature. Many of these indexes need parameters not always available and easy to acquire, such as grain size distribution (Liao et al., 2022) or landslide velocity (Swanson et al., 1986).

In this work, we propose a simple semi-automatic GIS-based mapping methodology to verify the damming susceptibility of river networks at national scale from existing and neo-formed landslides trough a geomorphological index. This activity research was carried out in the framework of the SFRARR Project ("*Strengthening Financial Resilience and Accelerating Risk Reduction in Central Asia*") as a part of a multi-hazard approach (Peresan et al., 2023).

The proposed mapping methodology represents an innovation in terms of application simplicity, availability of data and of extension of the analysed area, bringing new information on the damming hazard in the Central Asia regions where the landslide susceptibility is quite high (Rosi et al., 2023) and a set of input data required for the methodology application were available.

## 2    Study area

Central Asia is a region of vast diversity encompassing high mountain chains, deserts, and steppes (Figure 1). The southern and eastern parts of the region are predominantly occupied by the mountainous areas of Djungaria, Tien Shan, Pamir, Kopetdag, and a small part of Western Altaj, with peaks exceeding 7,000 m above sea level (a.s.l) (Strom, 2010). These intraplate mountain systems, developed in the Cenozoic as a result of the India-Asian collision, is located between the Tarim Basin and the Kazakh Shield (Molnar and Tapponier 1975, Abdrakhmatov et al., 1996; 2003; Zubovich et al., 2010; Ullah et al., 2015). This study focusses the attention on the territories of Central Asia that includes Turkmenistan, Kazakhstan, Kyrgyz Republic, Uzbekistan, and Tajikistan, covering a surface of more than 4·10$^6$ km$^2$. Mountain building began in the Oligocene (Chedia, 1980) or later (Abdrakhmatov et al., 1996), resulting in a complex system of basement folds interrupted by several thrusts and reverse faults with lateral offset of important amounts (Delvaux et al., 2001).
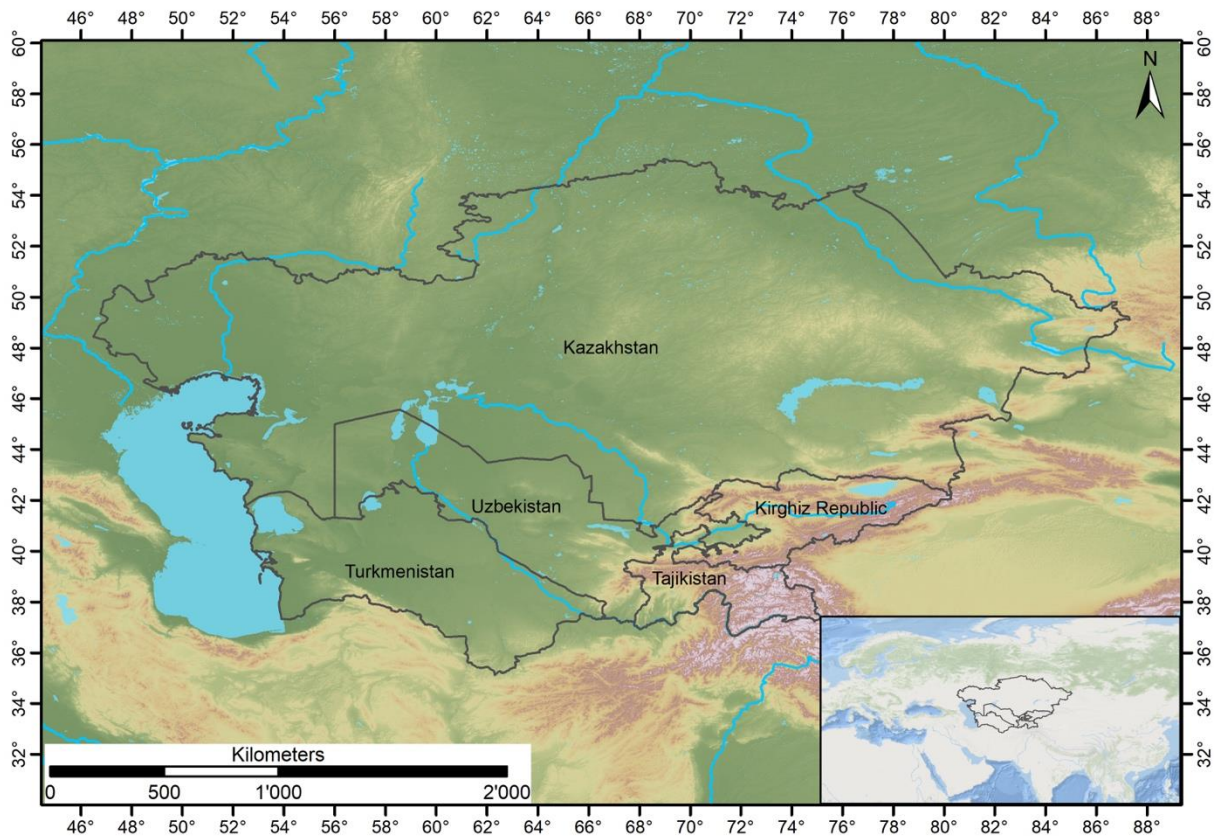
107 **Figure 1. Geographical framework of the study area.** Lake's polygons from Esri, Garmin International, Inc.;
108 topographic base from NASA's SRTM project (Farr and Kobrick, 2000).

109 The mountain belts contain several regional fault zones (Figure 2), and others cross the mountain systems with a
110 NW-SE axis (Trifonov et al., 1992). Paleozoic crystalline rocks form, for the most part, the mountain ridges which
111 correspond to a neotectonic anticline and are separated by tectonic depressions, with lenticular or linear shapes.
112 These intermountain depressions host the primary river valleys and are filled by Neogene and Quaternary deposits,
113 principally sandstones, siltstones interbedded by gypsum, and conglomerates (Strom and Abdrakhmatov, 2017).
114 Lithologies from Mesozoic and Paleogene are characteristic of the areas at the foot of mountain ranges (Figure 2).
115 This main deeply incised river network, fed by glaciers, snowmelt water and rain, is linked by narrow deep gorges
116 up to 1-2 km deep (Strom and Abdrakhmatov, 2018) and is the origin of most of the rivers in Central Asia.
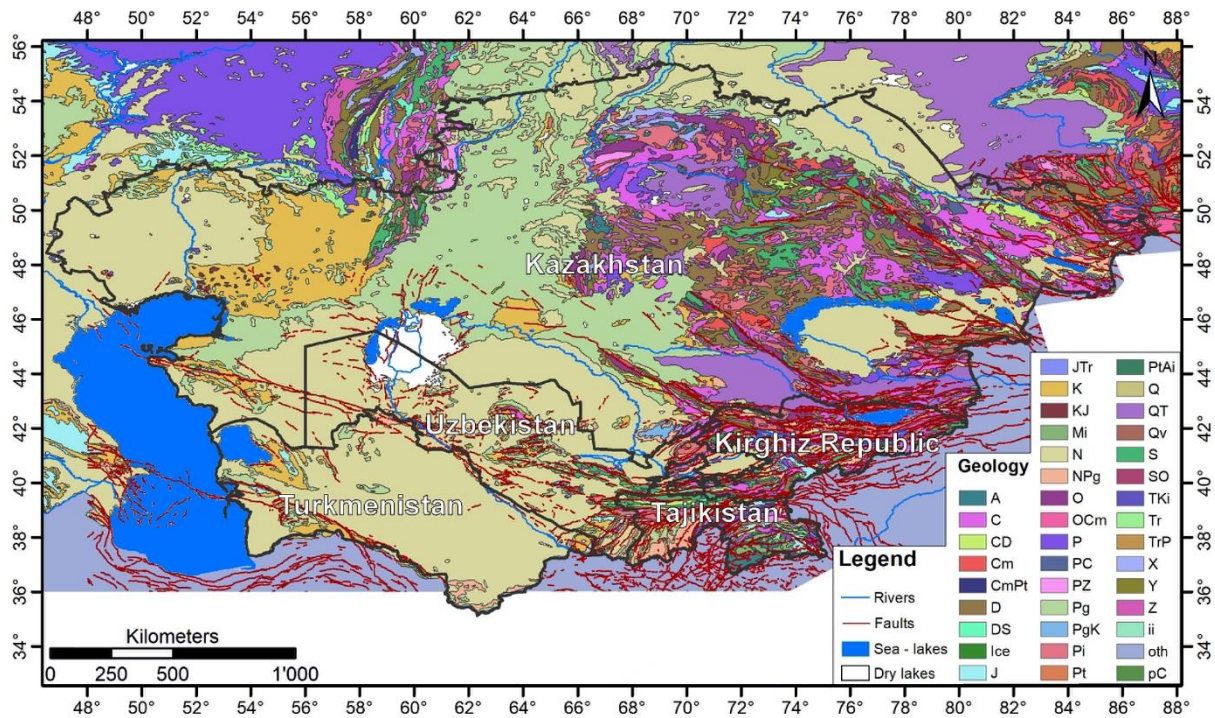
Figure 2. Geological map of the area. Geological formation data are from the United States Geological Survey (USGS) (Persits et al., 1997, https://doi.org/10.3133/ofr97470E, for the legend), faults are from the Active Faults of Eurasia Database (AFEAD) (Styron and Pagani, 2020, https://doi.org/10.1177/8755293020944182).

The retreat and shrinkage of glaciers in Central Asia regions induced by the global warming produce a seasonal variation in river discharge and consequently an increase of its induced hazards such as Glacial Lake Outburst Floods (GLOFs) (Falátková, 2016), resulting in countless losses of human life and destroyed infrastructure (Kropáček et al., 2021; Petrov et al., 2017; Wang et al., 2013). The high seismicity, frequent floods and a complex geological and topographical structure (such as lithological predisposition, faulting zones, steep slopes) contribute to predispose the region to frequent landslides which can potentially obstruct the narrow valleys of the mountain ranges and in turn be the cause of chain risks (CAC DRMI, 2009; Havenit et al., 2017).

**3      Materials and Methods**

The Morphological Obstruction Index (MOI) (Tacconi Stefanelli et al., 2016) is a bivariate index able to evaluate the potential hazard posed by landslide dams that requires only simple morphometrical parameters which are easily extracted from common Digital Elevation Models. The MOI is based on the interpolation of 351 documented cases and has been used in several studies, such as in Italy and Peru (Tacconi Stefanelli et al., 2016; 2018), to assess landslide damming susceptibility showing better results than others popular indexes (Swanson et al., 1986). This empirical index is a useful tool for identifying high-risk areas and for prioritizing mitigation efforts in landslide-prone regions.

The MOI is calculated by dividing the volume of the landslide, $V_l$ (m$^3$), by the width of the river valley, $W_v$ (m), at the dam location.

138 $$MOI = log\left(V_l / W_v\right) \qquad (1)$$

139 The MOI is based on the principle that the higher the ratio of the landslide volume to the river width, the greater

140 the potential for dam formation. It is important to point out that river width, $W_v$, shall be defined as the width of

141 the river valley which can potentially be obstructed creating a dammed lake and not of just the channel where the

142 river flows, as is often misinterpreted, although in narrow mountain valleys these often coincide.

143 Landslide dams analyzed by the index can be grouped within three evolutionary classes: formed (the red area,

144 where the plotted landslides have completely blocked their river), not formed (the blue area, where only cases of

145 unobstructed rivers are found) and of uncertain evolution (the purple area, in which both cases of formed and

146 unformed dam can be found). The limits of these domains are depicted by two lines, the lower red "Non-formation

147 line" and the upper blue "Formation line" (Figure 3) obtained by the interpolation of the cases analyzed by Tacconi

148 Stefanelli et al. (2018).
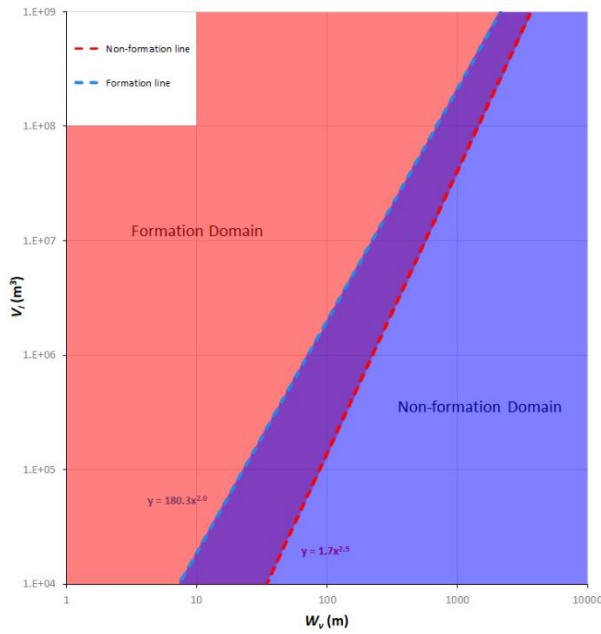
149

150 **Figure 3. Schematic plot of the non-Formation line and Formation line.**

151 The equation of the former is expressed as follows:

152 $$V_l' = 1.7 \cdot W_v^{2.5} \qquad (2)$$

153 Where $V_l'$ is the "Non-formation volume" and is the minimum landslide volume able to potentially block a river

154 with a given width $W_v$. Smaller volumes cannot completely dam the river. The latter expression draws the upper

155 limit for not formed dams and is expressed as follows:

156 $$V_l'' = 180.3 \cdot W_v^2 \qquad (3)$$

157 Where $V_l''$ is the "Formation volume", is the minimum landslide volume able to dam the river valley, with a

158 confidence of 99%, and the inferior boundary of the Formation domain (which includes only formed dams).

159    Intermediate cases that fall between the two lines cannot be confidently identified as formed or unformed and are

160    therefore classified as having uncertain evolution.

161    As originally proposed by Tacconi Stefanelli et al. (2020), these two equations, Eq.(2) and (3), can be used to

162    apply a simple semi-automatic methodology in order to verify at basin scale the damming susceptibility from

163    existing and neo-formed landslides. The following semi-automated procedure, inspired by the one of Tacconi

164    Stefanelli et al. (2020) of which this represents an improvement, is applied on a national scale and can be

165    reproduced entirely in a GIS (Geographic Information System) environment. However, the method, being initially

166    designed for analysis at basin/region scale, applied to such a small scale (national) will not be able to provide

167    detailed information. For this reason, this study represents a preliminary phase of investigation which will allow

168    to concentrate further detailed analysis on the areas identified as more critical.

169    Within an even medium-long time interval the valley width in each river stretch does not change significantly and

170    can be considered an immutable factor in the MOI equation (Eq.(1)). Starting from this assumption, along with

171    Eq. (2) and Eq. (3), if the average river width $W_v$ of each river stretch can be assessed, the two threshold landslide

172    volumes $V_l$' (Non-formation volume) and $V_l$'' (Formation volume) can be estimated for each river stretch.

173    Landslides that cause river obstruction are in many cases reactivations of ancient movements that are still in a

174    condition of partial instability and that have not reached a potential equilibrium reaching the valley floor.

175    Therefore, with a landslide inventory it is possible to assess, with some assumptions and simplifications, which

176    among the mapped landslides are able to dam the river section. Each landslide that is not already laying in the

177    valley floor with a volume bigger than V' and V'' are identified as potentially prone to block the river in the future

178    in that point. Then, a "Map of Damming Susceptibility" for reactivation of existing landslides can be generated.

179    The likelihood prediction for new landslides, with volume bigger than $V_l$' and $V_l$'', is a much more difficult task

180    as the volume is a complex value to be estimated (Catani et al., 2016). The exceeding probability of landslide

181    volume used by Tacconi Stefanelli et al. (2020) was reached thanks to the knowledge of the alpha exponent of the

182    statistical frequency distribution of the landslide volumes in the whole study area. To achieve this, a database of

183    landslides with a very high number of events (tens or even hundreds of thousands) should be available (Catani et

184    al., 2016), which in our study area unfortunately is not. To have an assessment of the damming susceptibility for

185    neo-formed landslides the two volume threshold values, evaluated for all the river networks, can be used as well.

186    After estimating the river width of every river stretches, the $V_l$' and $V_l$'' values of each of them can be computed

187    through the corresponding two equations. In this way there will be two reference values to be able to assess whether

188    the volume of a new landslide can potentially obstruct an affected river stretch.

189    The input data needed for the procedure are a Digital Elevation Model, a vector layer of the river network, and an

190    updated landslide inventory. The data quality and resolution such as the landslides inventory completeness, the

191    river network reliability and the DEM's pixel size heavily affect the quality of the result (Tacconi Stefanelli et al.,

192    2020). Thus, it was decided to use the DEM with the higher resolution freely available from the NASA's SRTM

193    project (Far and Kobrick, 2000) with a 1 arc-second, or about 30 meters of resolution. The river network came

194    from Coccia et al. (2023). The latter input data is a database of 8910 landslides, that is a compilation of several

different inventories collected through decades of field surveys, studies and remote sensing analysis in the study area, shown in Figure 4.

Hereafter the detail of each inventory:

- The "Rockslides and Rock Avalanches of Central Asia" (Strom and Abdrakhmatov, 2018): an inventory including more than 1000 of very big (>=1 Mm$^3$) rockslides and rock avalanches, covering central Asian countries (excluding Turkmenistan and Altai) and also Chinese Tien Shan and Pamir, and Afghan Badakhshan. Collected in decades of field survey and analysis of aerial/satellite imaging, it includes also information on morphometric parameters (runout, area), dammed lakes, head-scarps, and quantitative characteristics (such as area, volume) for about 600 cases.

- The "Tien Shan landslide inventory" (Havenith et al., 2015a): is the biggest database in the study area. Assembled through field work, remote sensing and geophysical data interpretation, it includes the elements of the previous inventory alongside other smaller landslides in soft sediments (Havenith et al. 2006a; Schlögel et al., 2011) for a total of 3,462 landslides polygons, including information on landslide length and area.

- The "Multi-temporal landslide inventory for a study area in Southern Kyrgyz Republic derived from RapidEye satellite time series data (2009 – 2013)" (Behling et al., 2014; 2016; Behling and Roessner, 2020), includes 1,582 landslide polygons mapped from multi-sensor optical satellite time series data (from 1986 to 2013) over an area of 2,500 km$^2$ in the Fergana valley rim in southern Kyrgyz Republic, and include information on landslide activity (area and year of trigger).

- The "Tajikistan landslide database" produced by the Institute of Water Problems, Hydropower, Engineering and Ecology of Tajikistan (IWPHE), with 2,710 landslide polygons and 114 landslide-prone areas, including information on landslides length and area.

- The Institute of Seismology of the Academy of Science of Uzbekistan (ISASUZ) provided an inventory which covers the Tashkent province composed by a point inventory (Niyazov, 2020) and a polygon inventory (345 landslide) digitized from the maps in Juliev et al., 2017.

219
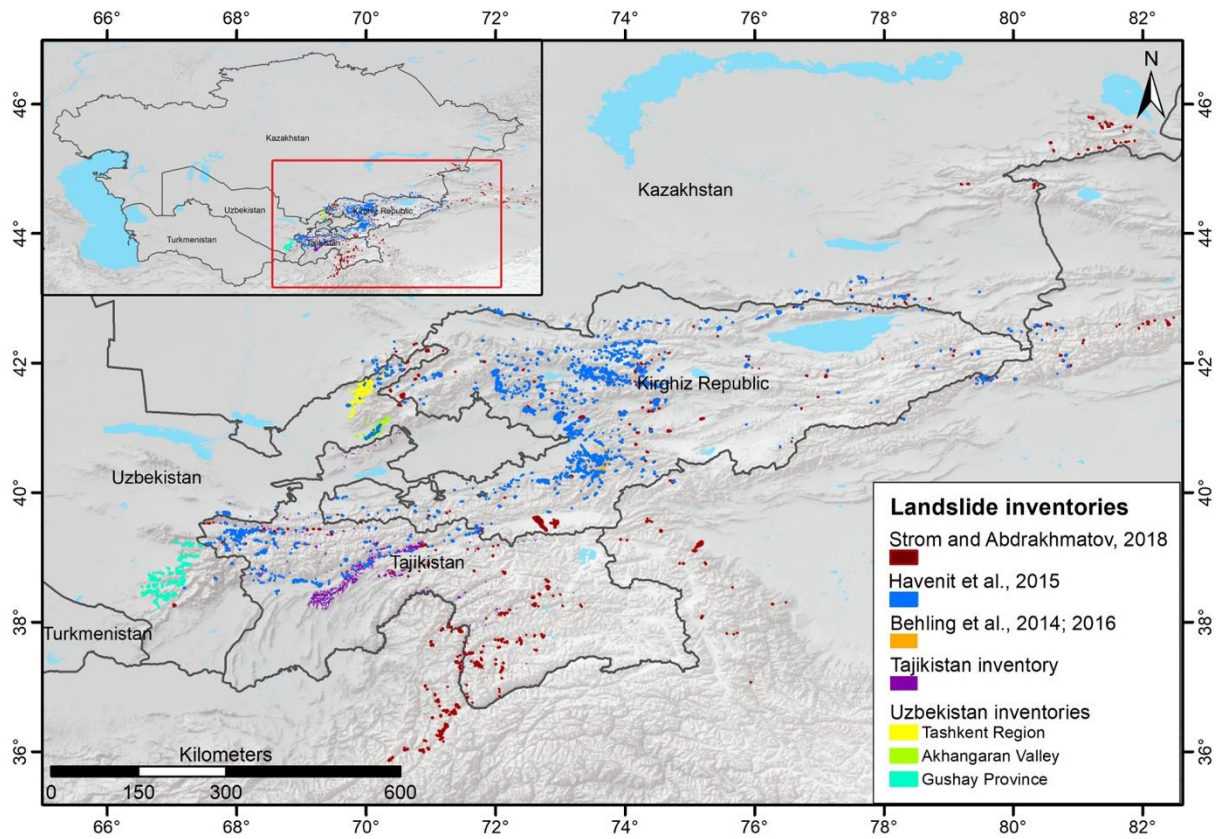
**Figure 4. Map of the landslide inventories in the study area.** Lake's polygons from Esri, Garmin
International, Inc.; basemap from Esri, USGS, NOAA.

The methodology adopted to obtain the maps of damming susceptibility, derived from Tacconi Stefanelli et al.
(2020), is summarized in the following main steps displayed in Figure 5. According to the literature (Swanson et
al., 1986; Fan et al., 2014; 2020; 2021; Tacconi Stefanelli et al., 2015; 2018), river obstructions occur in most of
the time within hilly or mountainous areas and specially along steep slopes. Therefore, considering the extension
of the study area, in order to reduce the time of elaboration and improve the visualization of the results, in step I
of Figure 5 a series of unnecessary data were removed from the calculations during some preliminary operations.
For this reason, river that flow in flat areas (with less than 4° slopes) were not considered in the elaborations, since
their damming probability is certainly very low with an extremely wide valley width. Additionally, to have maps
easier to manage and display, the river network was split in 5 km long river stretches consecutive to each other.
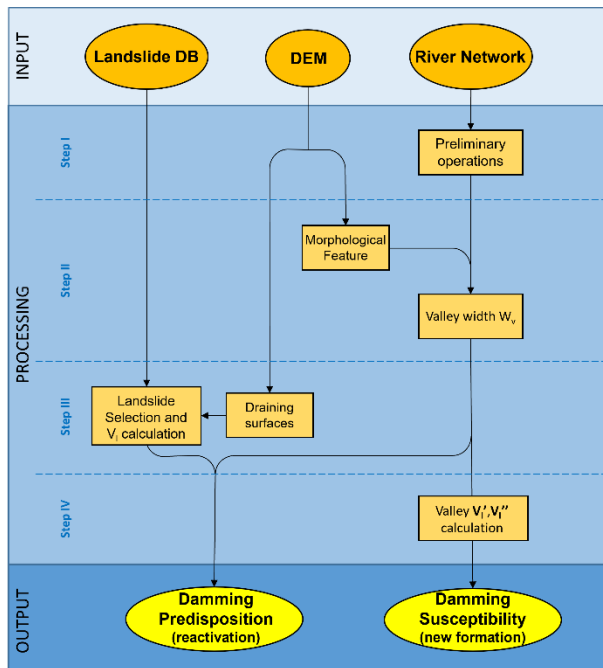
232 **Figure 5. Flow chart of the main steps of the mapping methodology.**

233 In applied geomorphology and natural science studies the analysis and characterization of the landscape has

234 evolved during the last decades with the increasing accessibility of remote sensing data and the development of

235 different algorithms able to automatically extract morphological features and landform information even at broad

236 scales (Drăguţ and Dornik, 2016; Maxwell and Shobe, 2022; Righini and Surian, 2018; Wang et al., 2010).

237 As already mentioned, the clear definition of the width of a river can be subjective and its measurement difficult

238 to repeat especially if performed by different operators. In step II of Figure 5, an objective automatic method to

239 extract morphometrical parameters have been chosen also for this reason. Wood (2009) implemented the

240 "*LandSerf*" software (already incorporated in SAGA GIS or QGIS software), designed to automatically classify

241 landforms from DEMs. Similarly for pattern detection and texture analysis within image processing, the software

242 extracts land-surface parameters (e.g., slope, aspect, and curvature) from DEMs through a multi-scale approach.

243 During these processing, the algorithm performs a classification of the landscape, grouping the landforms with

244 homogeneous morphometric characteristics (pits, channels, peaks, ridges, passes, and planes) as shown in Figure

245 6. Thanks to this algorithm of morphological forms analysis proposed by Wood (2009), the polygons representing

246 the morphological unit of the river valley can be automatically defined objectively even in a large area and

247 extracted.

248
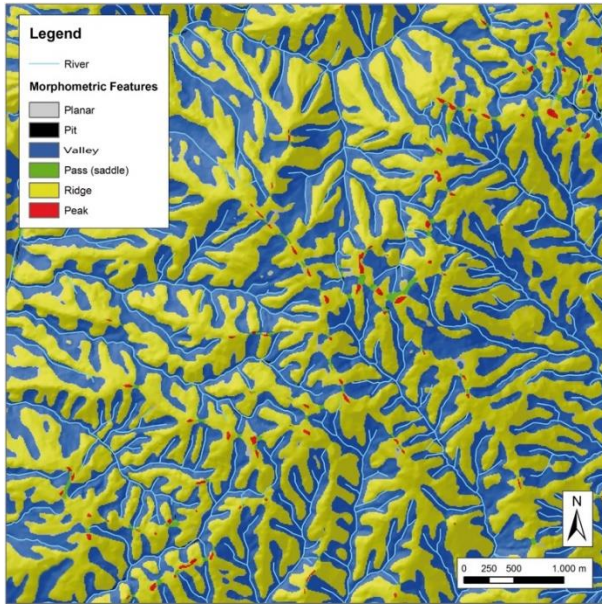
**Figure 6. Classification of the landscape into morphological classes according to Wood (2009) (modified from Tacconi Stefanelli et al., 2020).**

The effectiveness of distinguishing different morphological landforms of this automatic tool is greater in mountainous regions characterized by significant differences in elevation, compared to flat areas where distinctions between landforms are less evident. The accuracy of the output is directly correlated with the resolution of the DEM, which should ideally be about a few meters. Coarser resolutions result in landslide volumes with a corresponding level of uncertainty.

The following phase is to provide to each river stretch a value of a valley width, $W_v$. A series of 1 km long lines (hereafter "transects") are generated, perpendicular to the stretches of the river network, outdistanced by 500 meters apart from each other. The created river valley polygons are used to "cut" the transects and then to measure the distance between the two river valley borders through the length of the cut transects.

Next, the valley widths ($W_v$) for each segment of the river are determined by assigning them an average value based on N perpendicular transects, excluding the extreme values (maximum and minimum, respectively $W_{max}$ and $W_{min}$), as in the fallowing equation:

$$W_v = \left(\sum_{i=1}^{n} W_i - W_{min} - W_{max}\right) \frac{1}{n-2} \tag{4}$$

By utilizing an updated database of landslide polygons, in the step III of Figure 5 it is possible to determine if a reactivated landslide is big enough to cause a complete river blockage thanks to the comparison with the boundary volumes of $V_l'$ (below which a landslide cannot completely block the river) and $V_l''$ (above which the river valley is dammed for sure). A reactivated landslide should follow a downhill path akin to the flow of surface water. Within each slope, the drainage directions can be easily determined along the river network using a GIS software. Each mass movement can then be linked to the corresponding river stretch it would reach if reactivated based on their corresponding draining surfaces.

271 Since the information provided by the available inventories in the study area are not homogeneous and comparable,

272 for the computation of the landslide volume were chose to use the areas of the landslide polygons, since it is the

273 most common data. An experimental statistical relationship between areas and volumes was applied:

274 $$V_l = \varepsilon \cdot A_l^\alpha \tag{5}$$

275 where $V_l$ and $A_l$ are respectively the volume and the area of a landslide, $\varepsilon$ and $\alpha$ are respectively the constant and

276 the exponent of the power law describing the landslides volumes frequency distribution. Various experimental

277 relations of $\varepsilon$ and $\alpha$ have been employed for landslide volume calculations by researchers located in different

278 countries. After an evaluation of these relations in the study area, the parameter proposed by Guzzetti et al. (2009)

279 have been selected because of the number of the studied cases (667) and the magnitude range of the landslides

280 area investigated (from $10^1$ to $10^9$ m$^2$). The landslide volume computed using this procedure is based on some

281 approximations, since they use geometric simplifications, but it does still reflect the magnitude of the process. The

282 result of the computation in Figure 7 shows an almost bimodal distribution, in which most landslides (83%) have

283 moderate volumes, lower than 10 million m$^3$ (with 63% lower than 1 million m$^3$), but 4% have value higher than

284 100 million m$^3$.

285 Then, Table 1 is used to assign to each landslide of the inventory a classification based on the comparison with the

286 boundary volumes $V_l'$ and $V_l''$, with value of 2 if the calculated landslide volume, $V_l$, is bigger than $V_l'$ (or $V_l''$),

287 of 0 if it is smaller. For more caution, the $V_l$ values is increased by an arbitrary value of 20% ($V_l \cdot 1.2$) to avoid

288 any potential underestimation during volume estimation and even the possible increase of landslide size with the

289 reactivation due to the mechanism of material entrainment (Hungr and Evans, 2004). For each landslide, if the

290 computed boundary volume $V_l'$ (or $V_l''$) is bigger than the estimated landslide volume $V_l$, but smaller than $V_l \cdot$

291 1.2, then a classification value of 1 is attributed.

292 The damming susceptibility of each mapped landslide is assigned by integrating the two comparative classification

293 values from the intensity matrix illustrated in Figure 8. The matrix establishes five qualitative classes on a scale

294 of severity for damming susceptibility, ranging from Very Low (dark green) to Low (light green), Moderate

295 (yellow), High (orange), and Very High (red). The combination of a high $V_l''$ value (1 or 2) and a lower $V_l'$ value

296 (0 or 1) symbolized by gray squares is not possible according to their respective formulations.
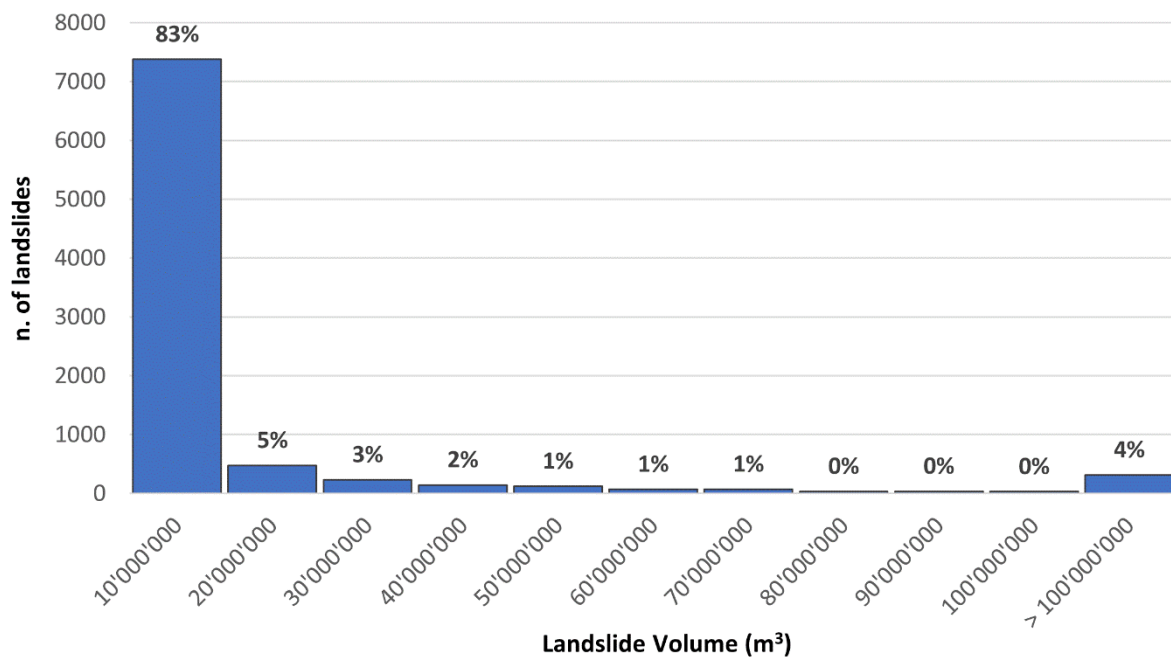
**Figure 7. Landslide volumes frequency distribution in the central Asia regions.**

**Table 1. Comparison table between landslide calculated volumes, $V_l$, with the boundary volume of Non-formation and Formation, $V_l'$ and $V_l''$(after Tacconi Stefanelli et al., 2020).**

|  | $V_l > V_l'$ $(V_l'')$ | $V_l < V_l'$ $(V_l'') < V_l * 1.2$ | $V_l < V_l'$ $(V_l'')$ |
|---|---|---|---|
| Classification Value | 2 | 1 | 0 |

**Figure 8. Predisposition matrix used for the assignment of the damming predisposition intensity to the mapped landslides (after Tacconi Stefanelli et al., 2020).**

Even if the proposed method is objective, it is certainly not free from uncertainties and errors. The 20% increase applied to mapped landslide volumes to reduce underestimation errors can in turn produce false positives for overestimation errors. While a false positive is preferable to a false negative (according to a principle of prudence), too many high-risk false positive cases "spread" an unreal risk throughout the area instead of concentrating it in sites of real risk. Therefore, it can be assumed that the landslide bodies which have previously reached the valley floor have already generated most of their effect on the river network (Strom, 2010) or have had no effect, spending their potential risk component. These landslides, also with a volume higher than $V_1'$ and $V_1''$ and therefore classified with Very High dam predisposition, even if reactivated probably will not produce any further effect in the future. For these reasons, it was decided to downgrade the classification of those landslides that intersect the river network by reducing its position of the classification of damming predisposition by one class.

Using the $W_v$ value for each river stretches estimated during the step III of Figure 5, in the last step (IV) the two boundary landslide volumes, namely "Non-formation volume" and "Formation volume" ($V_1'$ and $V_1''$), can be estimated by applying the equations of the "Non-formation" (Eq. (2)) and "Formation" lines (Eq. (3)). These two values can be used both to classify the damming susceptibility of the river network (for new landslides) and of the landslides inventory (for their reactivation). For the first case, the computed volume values $V_1'$ and $V_1''$ embody the required volumes of a new landslide to have a potential or certain (with 99% of confidence) obstruction for each river stretches.

## 4    Results

The mapping methodology was applied to all the studied territories of the Central Asia region in order to analyze and evaluate the results. Two smaller basins, the upper Pskem river and the Fergana valley, were selected to verify the reliability at a catchment scale of the results obtained from a methodology applied on a national scale. The assessment of damming predisposition on the available landslide inventory on the Central Asia regions is shown in the map of Figure 9, while a closer detail is reported in Figure 10 showing the Kyrgyz Republic territory. The number of landslides (644 cases) classified with Very High damming predisposition from the whole inventory before the class reduction due to the river intersection was unjustifiably and unreasonably large posing excessive concern and risk perception. After the change, this number decreased by 75% up to 166 cases, a high number but more reasonable concerning such a large area. In the class distribution of the damming predisposition the most frequent class is the Very Low, with 81% of the whole database, followed by the Low and High classes both with 6% and the remaining percentage divided among Moderate (5%) and Very High (2%).

This distribution is quite coherent with the landslide volumes frequency distribution since it is reasonable to associate landslides with very low volume (83%, shown in Figure 7) with those classified with very low susceptibility (81%). The landslides classified with the higher values of susceptibility (Moderate, High, and Very High with a total of 13%) instead do not only include landslides with higher volumes (more than 100 million m$^3$ representing 4% of the total), meaning that also even smaller landslides can potentially block narrow river stretches in these regions.

340
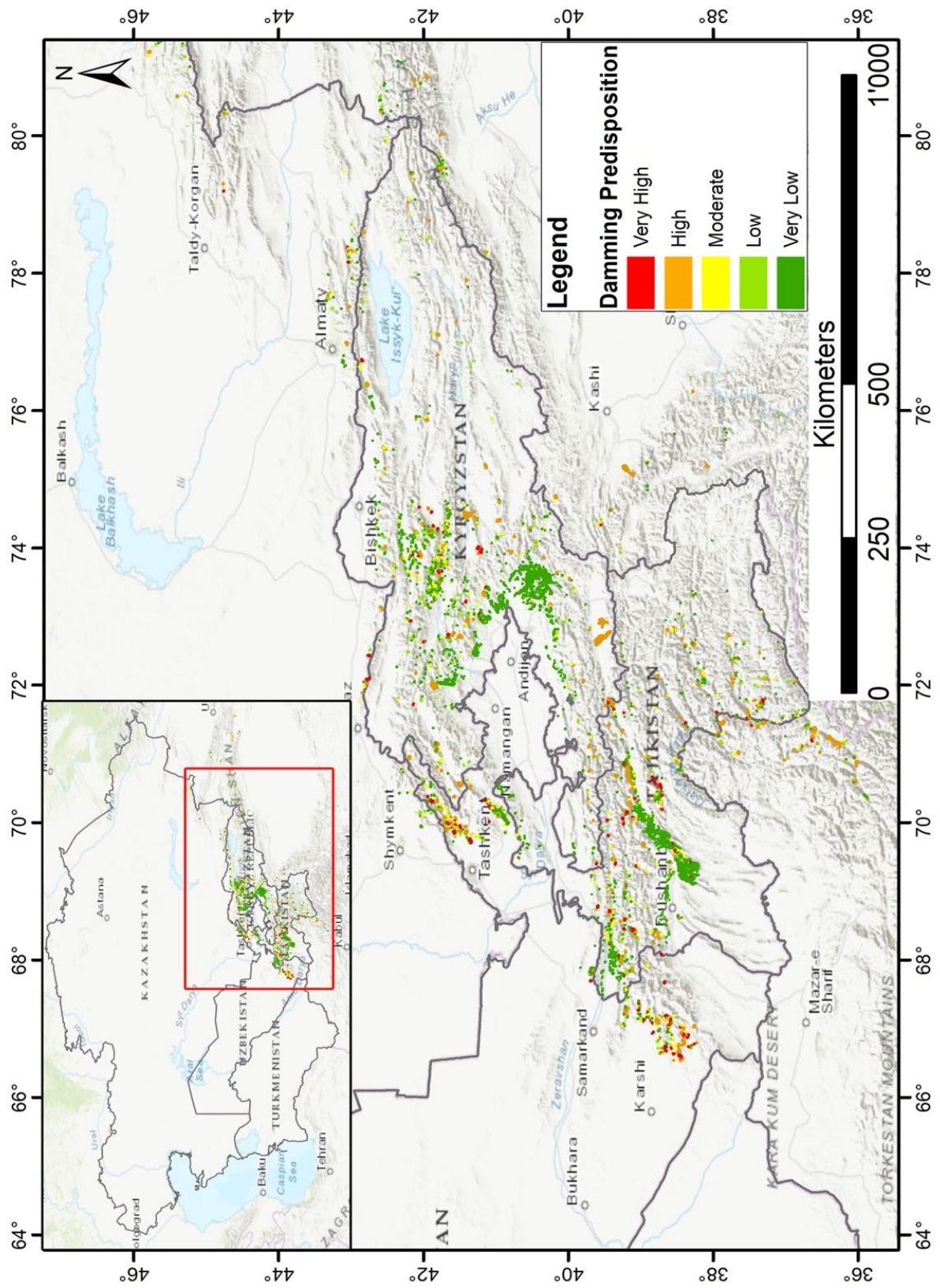
**Figure 9. Map of Central Asia Landslide Damming Susceptibility.** Basemap source: Esri, HERE, Garmin

342 Intermap, increment P Corp, GEBCO, USGS, FAO, NPS, NRCAN, GeoBase, IGN, Kadaster NL, Ordnance
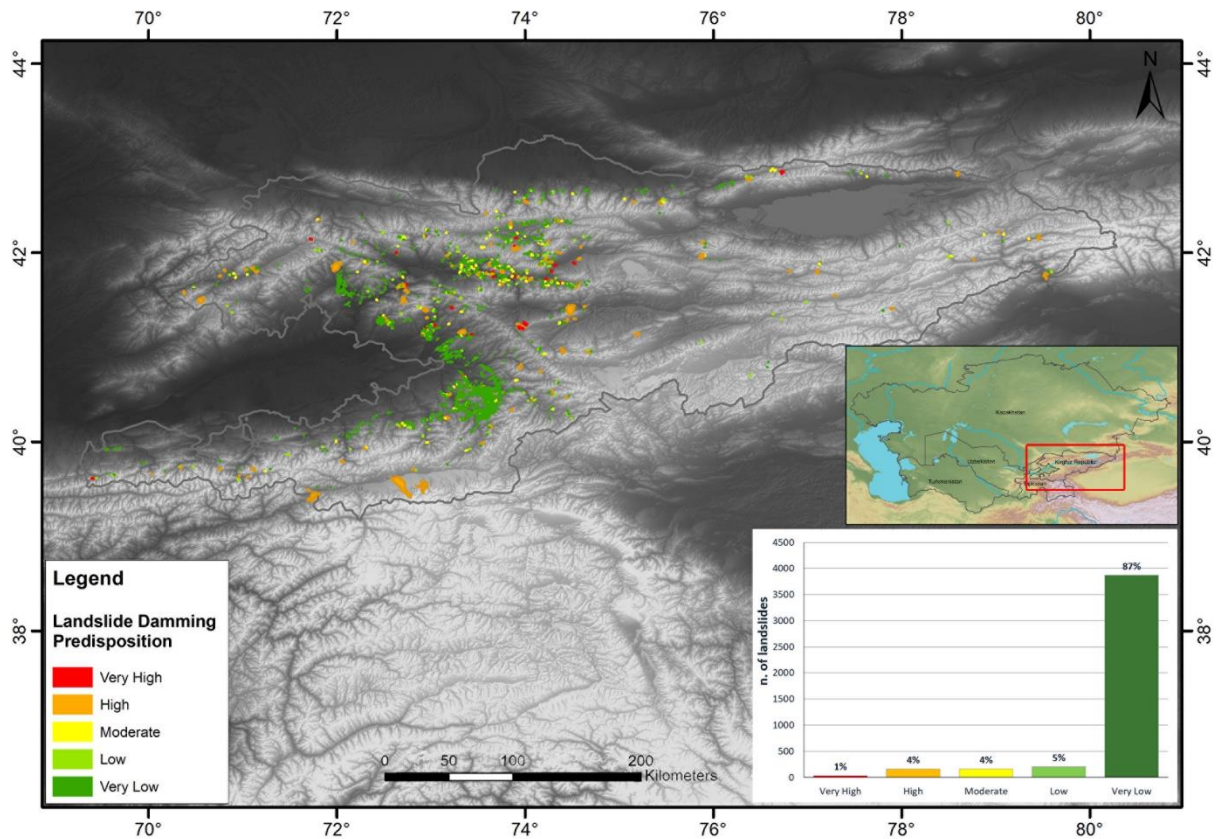
345

346    **Figure 10. Map of Damming Predisposition by landslides reactivation in Kyrgyz Republic territory.**
347    Topographic base from NASA's SRTM project (Farr and Kobrick, 2000).

348    Concerning the damming susceptibility caused by new landslides along all the river network in the study area, two

349    different maps of the river networks have been produced using the Non-formation and Formation volumes values.

350    Although counterintuitive at first glance, these maps provide complementary information. The former provides

351    the volumes of landslides that surely create an obstruction, while the latter the volumes below which it definitely

352    does not form. According to the preliminary steps of the described methodology, in the river stretches running in

353    flat areas (slope degree less than 4° representing the 88.4% of the entire river network) the analysis has been not

354    applied, due to the extreme unlikelihood that a complete obstruction will occur in such areas. The magnitude of

355    the damming susceptibility of the river networks has been classified in five classes and shown in Figure 11 and

356    Figure 13. The five volumes intervals describing damming susceptibility were decided according to general value

357    distribution of landslides volumes and an expert judgement. Since small landslides are more frequent than large

358    ones, as reported in Figure 7, the lower is the landslide volume required to realize an obstruction, the higher is the

359    magnitude. In the map of damming susceptibility related to the "Non formation", reported in Figure 11, 88.4% of

360    the regional river network lies in lowlands areas while Moderate and Low classes are the most frequent with 4.4%

361    and 5.8% respectively. This means that in most of the river stretches in the study area the minimum landslide

362    volume able to potentially dam the riverbed is between the limit values of the two classes, from 2,5 to 25 million

m$^3$. The following most frequent class is the Very Low with 0.8% and only a very small portion of the river stretches are classified as High and Very High with just 0.4% and 0.2% with a required landslide volume less than 2.5 million m$^3$. An example of close-up on the Tajikistan territory is reported in Figure 12.

Regarding the map of damming susceptibility related to Formation values, the map in Figure 13 shows slightly different results. The most frequent classes are the two lower ones, Low and Very Low with 4.4% and 6% respectively. Only just the 0.3% and 0.4% fall in the classes Very High and High damming susceptibility. A close-up on the Kyrgyz Republic is reported in Figure 14.

The results of the classification for the river networks of each state are shown in Figure 15. The landslides of Tajikistan, Kyrgyz Republic, Uzbekistan and Kazakhstan regions have been classified according to damming predisposition (Figure 15-a., Figure 15-d., Figure 15-g. and Figure 15-j.). In the Turkmenistan territory, it was not possible to assess any damming predisposition by landslides reactivation since the absence of any available landslide inventory. The results of Uzbekistan and Kazakhstan regions (Figure 15-g. and Figure 15-j.) are a bit different from Kyrgyz Republic and Tajikistan regions due to the different availability of landslide inventories and a different orographic and valleys morphology of the formers national territories. As already mentioned, for a clearer comprehension of the damming susceptibility classification of the river network at the national level, the river stretches flowing in lowlands have not been considered in the analysis. Concerning the Damming Susceptibility of Non-Formation (Figure 15-b., Figure 15-e., Figure 15-h., Figure 15-k. and Figure 15-m.), the most frequent are Low and Moderate classes, followed by Very Low class. Fortunately, only very few river stretches have been classified as Very High and High. For the Damming Susceptibility of Formation (Figure 15-c., Figure 15-f., Figure 15-i., Figure 15-l. and Figure 15-n.) most of the rivers fall into Very Low and Low classes, followed by Moderate class. Also in this case, only very few river stretches have been classified as Very High and High. The results of the Tajikistan territory are quite similar to the Kyrgyz Republic and Uzbekistan with which it shares a similar orographic distribution and morphology of the territory. Turkmenistan and Kazakhstan show a slightly different distribution with higher percentage on Moderate class in the Damming Susceptibility of Non-Formation and Low class in the damming susceptibility of Formation.
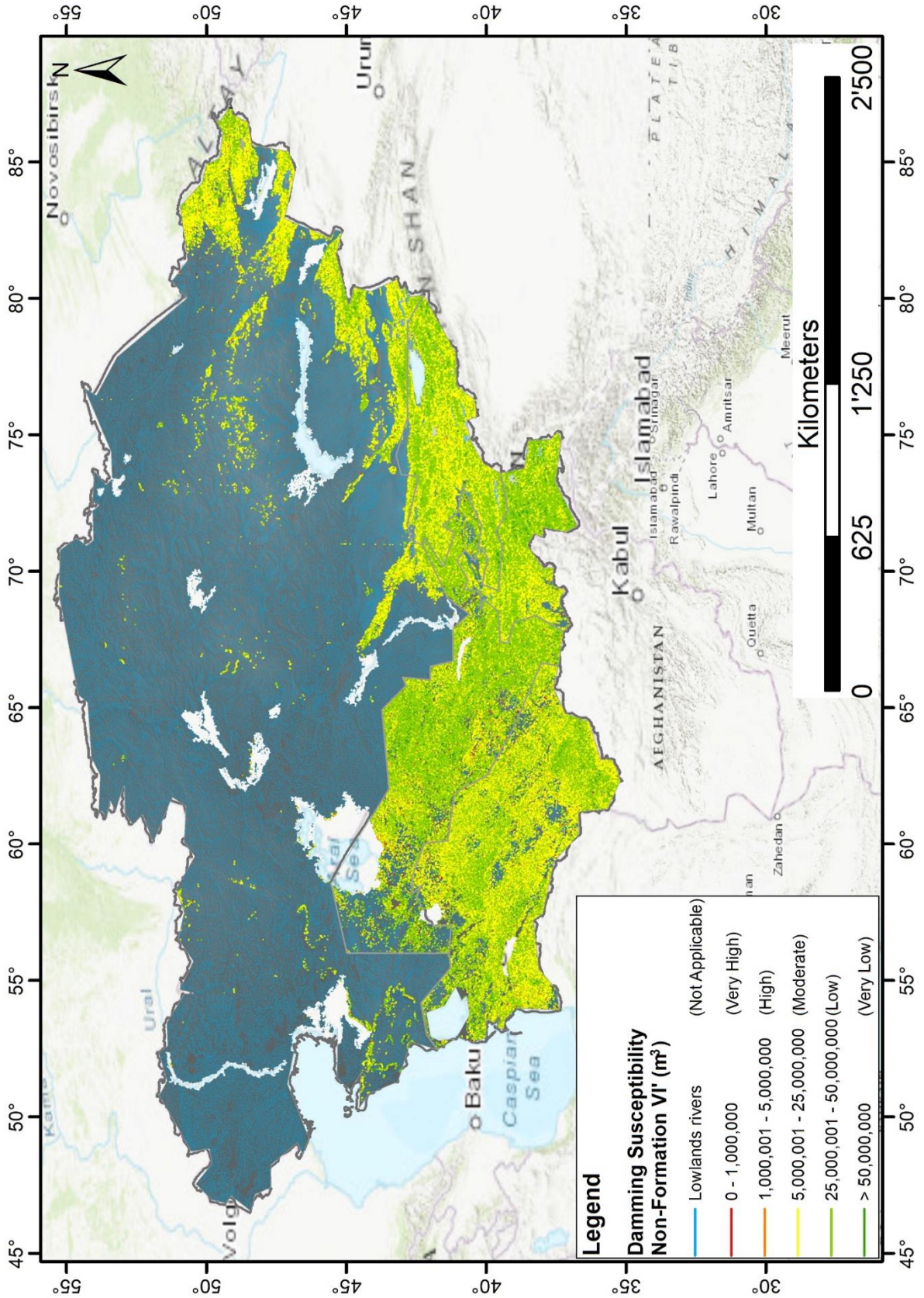
**Figure 11. Damming susceptibility map of non-formation of river stretches by new landslides in the region.**

River network database from Coccia et al. (2023). Basemap source: Esri, HERE, Garmin Intermap, increment P
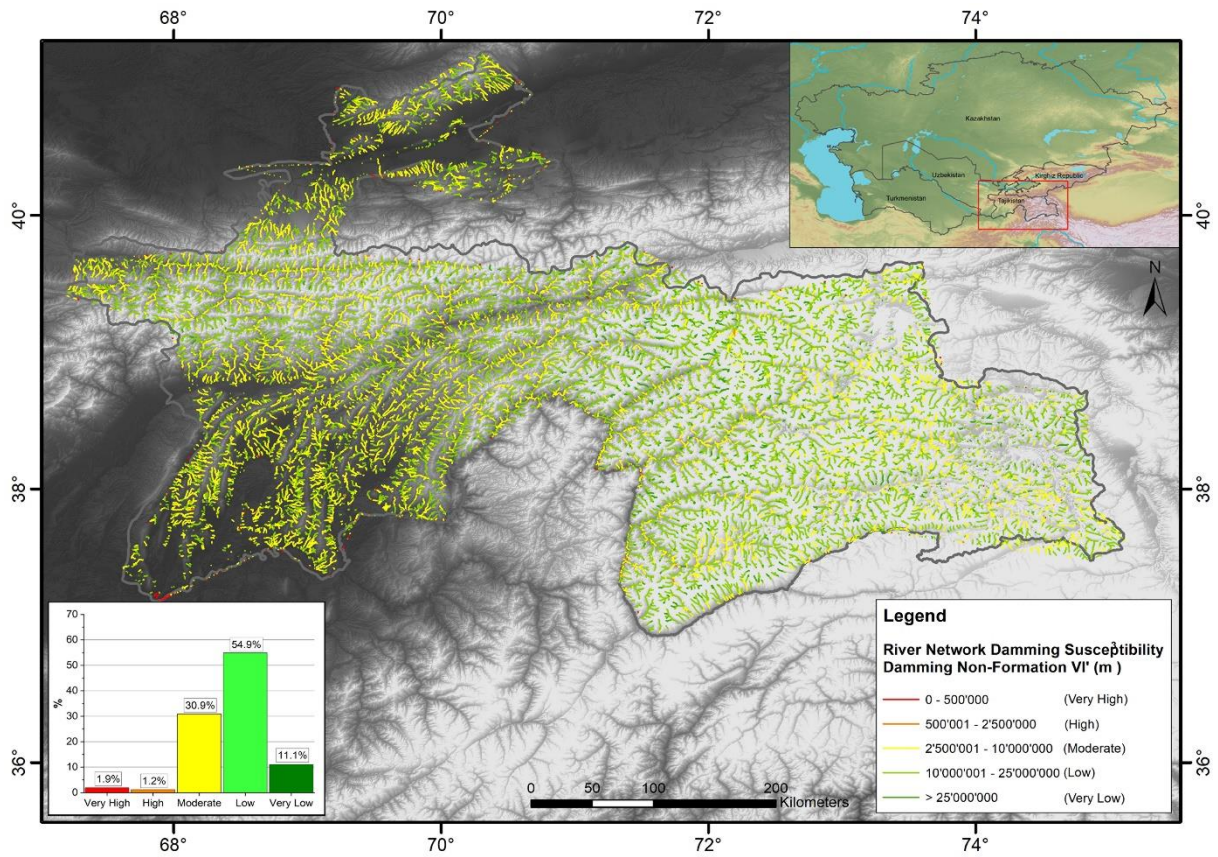
**Figure 12. Damming Susceptibility Map of non-formation of river stretches by new landslides in Tajikistan.** River network database from Coccia et al. (2023). Topographic base from NASA's SRTM project (Farr and Kobrick, 2000).
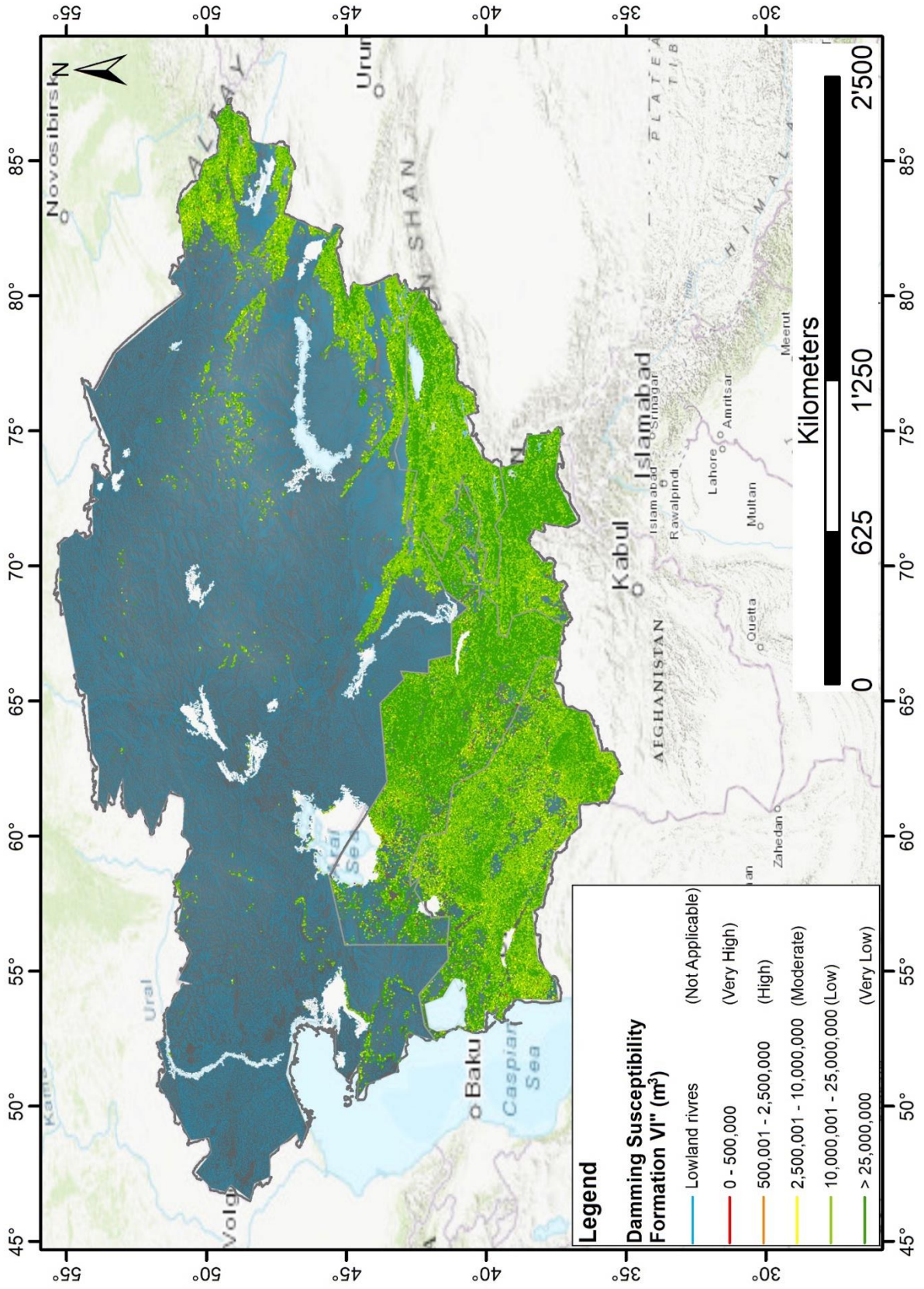
**Figure 13. Damming Susceptibility Map of Formation of river stretches by new landslides in the region.**

River network database from Coccia et al. (2023). Basemap source: Esri, HERE, Garmin Intermap, increment P
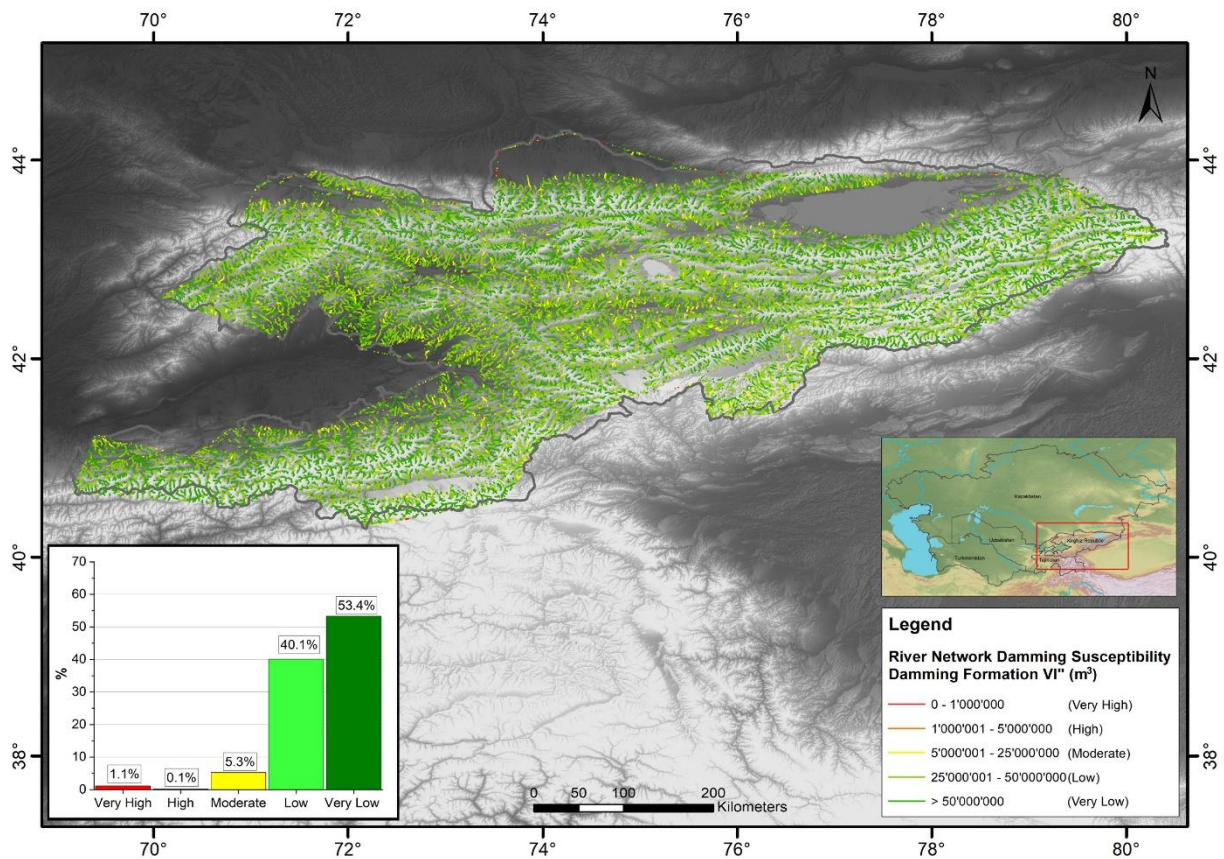
**Figure 14. Damming Susceptibility Map of formation of river stretches by new landslides in the Kyrgyz Republic territory.** River network database from Coccia et al. (2023). Topographic base from NASA's SRTM project (Farr and Kobrick, 2000).
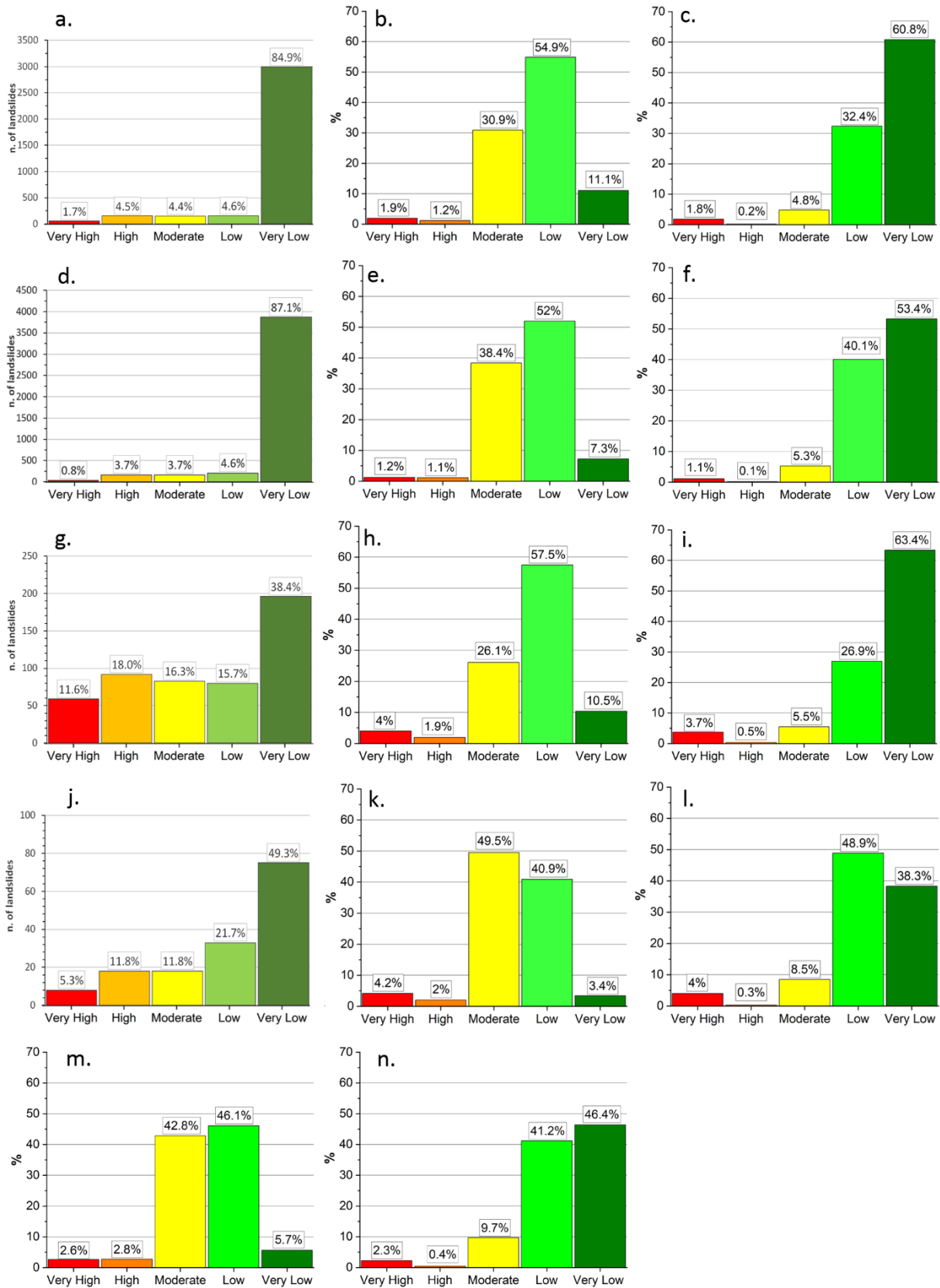
406

407 **Figure 15. Classes distribution of Damming Predisposition for landslides reactivation, Damming**
408 **Susceptibility of Non-Formation and Formation for new landslides, in Tajikistan (a.), (b.) and (c.), in Kyrgyz**

## 4.1 Upper Pskem river valley (Uzbekistan)

The Pskem river, locate in the Tashkent region of Uzbekistan, is a right-hand tributary of the Chirchik River that is the feeder of the Syr Darya river basin (in the Western Tien-Shan). The river originates from the confluence of the Maidantal and Oygaing rivers and is one of the main tributaries of the Charvak Lake (Semakova et al., 2016). This artificial lake is central for the local economy for its functions as reserve for fishing and water, as well as a source of hydroelectric energy and because of that various villages arise around it and downstream. The formation of a natural obstruction and an upstream impoundment in the Pskem basin could be a serious threat due to the possible instability of the earth dam and for the possible catastrophic cascade effects that its collapse could have downstream on the artificial basins and their 168 meters high earthfill dam.

With a careful observation of the map of Damming Predisposition by landslides reactivation in the lower Pskem basin in an area of 443 km$^2$ (Figure 16), some of the 53 mapped landslides should be subjected to further study. Among all, most landslides were classified with a Very Low and Low predisposition value, respectively 21 and 11 cases (39.6% and 20.8%), and only 4 landslides with a Very High value (7.5%), 10 with High (18.9%) and 7 with Moderate (13.2%). Landslides named A, B, C, D and E in Figure 16, if reactivated will potentially cause an obstruction of the main river section of the Pskem, being classified the first three and the latest two respectively with High and Very High damming predisposition. As shown in Table 2, the volumes of all these landslides are way bigger than the boundary volume of Non-Formation and Formation from Figure 17 and Figure 18. It is important to notice that the landslides A, B and C are laid down in the valley floor, meaning that in the past they had probably already dammed the river in that point, and the classification of their damming predisposition have been reduced by one, from Very High to High. Due to the considerable volumes of the landslides in the basin and the presence of landslides that have probably already blocked the river in the past, this relatively small area is certainly worthy of attention.

**Table 2. Landslides volumes and damming parameters W$_v$, V$_l$', V$_l$" of the landslides in Figure 16 computed using the described method.**

| Landslide | V$_l$ – Landslide volume (m$^3$) | W$_v$ – River Width (m) | V$_l$' – Volume of Non-formation (m$^3$) | V$_l$" – Volume of Formation (m$^3$) |
|---|---|---|---|---|
| A | 200.000.000 | 300 | 2.600.000 | 16.200.000 |
| B | 12.000.000 | 235 | 1.500.000 | 10.000.000 |
| C | 34.000.000 | 318 | 3.000.000 | 18.200.000 |
| D | 73.000.000 | 513 | 10.100.000 | 47.400.000 |
| E | 61.000.000 | 575 | 13.500.000 | 60.000.000 |

435
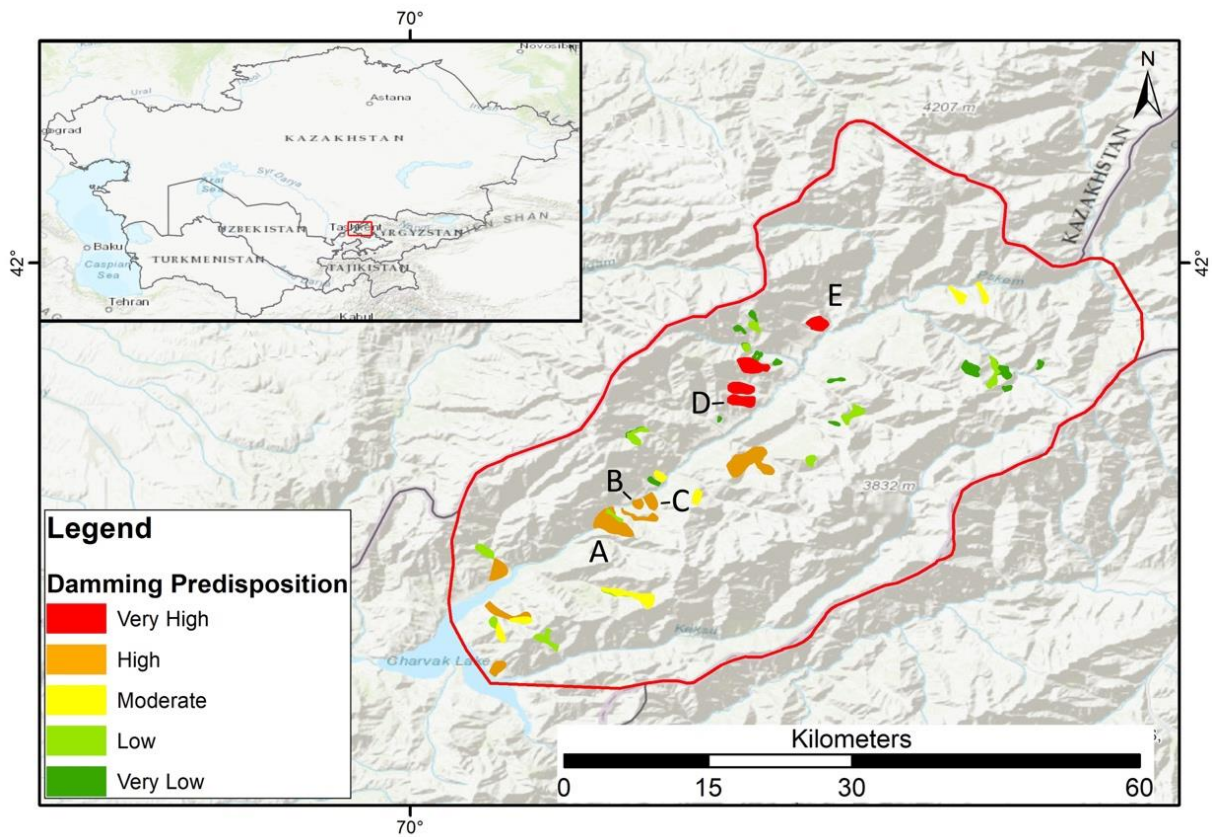
**Figure 16. Map of Damming Predisposition by landslides reactivation in the lower Pskem basin.** Basemap
source: Esri, HERE, Garmin Intermap, increment P Corp, GEBCO, USGS, FAO, NPS, NRCAN, GeoBase, IGN,
Kadaster NL, Ordnance Survey, Esri Japan, METI, Esri China (Honk Kong), © OpenStreetMap contributors, and
the GIS User Community.

The obstruction of the Pskem river by one of these landslides would cause an upstream impoundment with a
surface from 2 to 10 km² or more, depending on the dam position and height. The dam collapse could release a
catastrophic flooding wave with destructive effects in the downstream areas. In the worst scenario, even the
earthfill dam located few kilometers downstream could be seriously damaged with unpredictable effects. Since the
reliability of this mapping method is strictly correlated to the quality of the input data, when the used DEM has a
coarse resolution, in similar cases of possible risk to people's life it is always advisable to do a second "manual
check" even using some free satellite imaging services like Google Earth. In fact, when the DEM resolution is too
rough, the GIS tool used in this methodology to evaluate the extension of the riverbed morphologic unit can
produce inconsistent and incorrect results, causing improper damming susceptibility evaluations. The results of
the measurements on Google Earth orthophotos in Table 3 show that the difference between the river width values
calculated with the mapping method ($W_v$) and those measured on Google Earth ($W_{vGE}$) can in some cases be
substantial modifying the calculated boundary volumes V' and V'', although in this case they do not modify
drastically the final classification of the five landslides.

The river network of the upper Pskem valley have been also classified producing the maps of Damming
Susceptibility of Non-formation and Formation (Figure 17 and Figure 18 respectively). Concerning the Damming

455 Susceptibility Map of Non-formation (Figure 17), the most frequent are Low and Moderate classes with 65.1%

456 and 22.6% respectively, followed by Very Low class with 11.1%. Only just 1.3% have been classified as High and

457 0.0% as Very High. For the Damming Susceptibility Map of Formation (Figure 18) most of the rivers fall into

458 Very Low and Low classes with 69.8% and 27.7%, followed by Moderate class with 2.1%. Only 0.4% have been

459 classified as High and 0.0% as Very High.

460 **Table 3. Damming parameters $W_{vGE}$, $V_l'_{GE}$, $V_l''_{GE}$ of the landslides in Figure 16 computed with Google**

461 **Earth observation.**

| Landslide | $W_{vGE}$ – River Width (m) | $V_l'_{GE}$ - Volume of non-formation (m$^3$) | $V_l''_{GE}$ - Volume of Formation (m$^3$) |
|---|---|---|---|
| A | 415 | 6.000.000 | 31.000.000 |
| B | 310 | 2.800.000 | 17.300.000 |
| C | 260 | 1.800.000 | 12.100.000 |
| D | 530 | 11.000.000 | 50.000.000 |
| E | 450 | 7.300.000 | 36.500.000 |

462

463 The general damming susceptibility of the valley is low but a singular river stretch, marked by a black circle in

464 Figure 17 and Figure 18, classified with High susceptibility in both maps should be carefully evaluated. This river

465 part is clearly noticeable in the middle of the area along the main river path, a bit upstream from the landslides

466 named B and C. The high classification values mean that geographically in that point the valley width undergoes

467 a shrinkage and for this reason even a relatively small landslide generated from the surrounding slopes can create

468 an obstruction, therefore it would be worthy of a more detailed investigation.

469
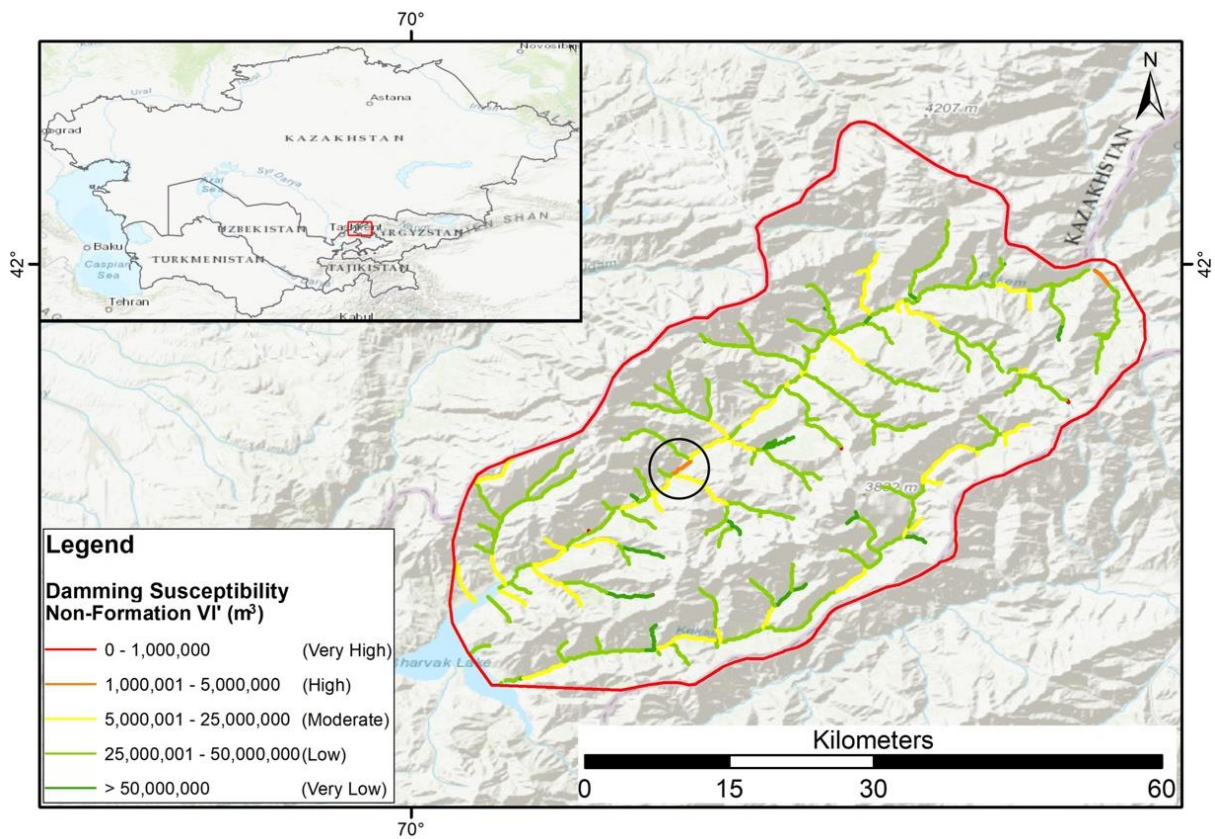
**Figure 17. Damming Susceptibility Map of Non-formation of river stretches by new landslides in the lower Pskem basin. The black circle highlights a river stretch with unusually high values.** River network database from Coccia et al. (2023). Basemap source: Esri, HERE, Garmin Intermap, increment P Corp, GEBCO, USGS, FAO, NPS, NRCAN, GeoBase, IGN, Kadaster NL, Ordnance Survey, Esri Japan, METI, Esri China (Honk Kong), © OpenStreetMap contributors, and the GIS User Community.
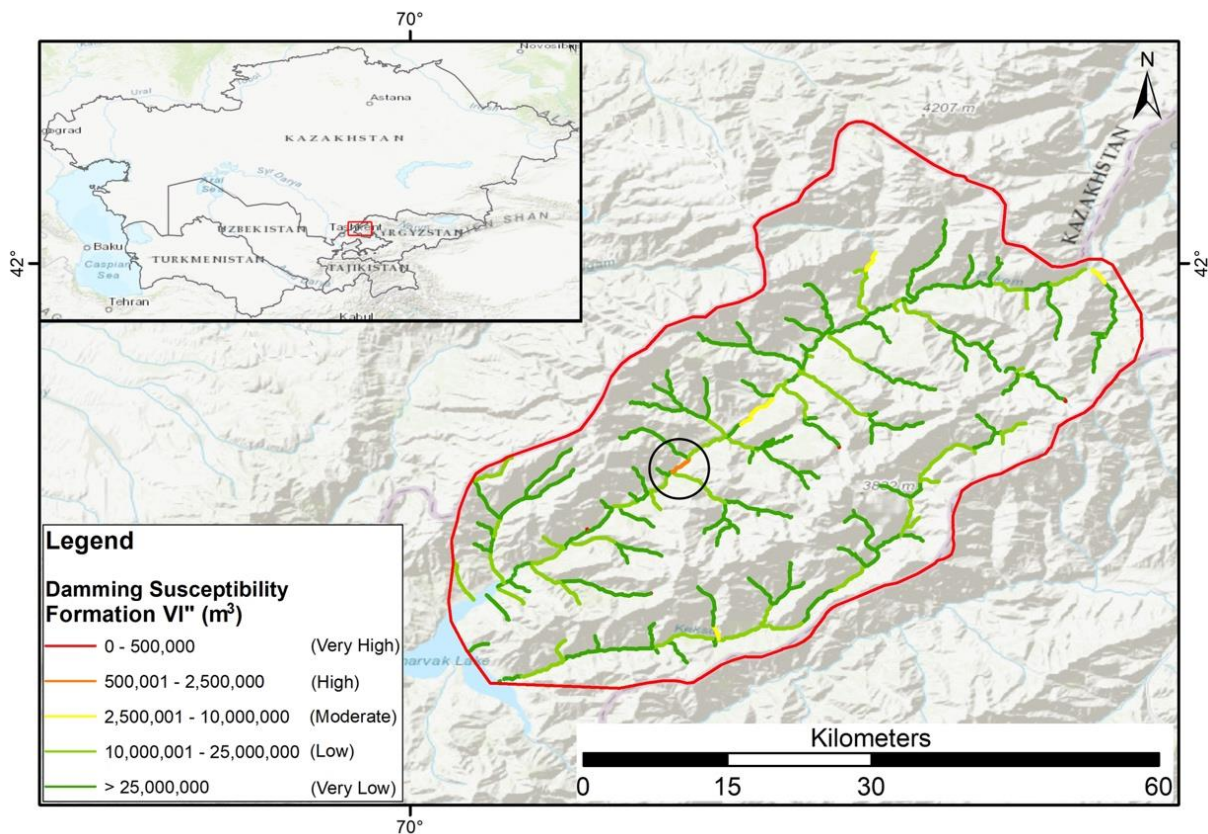
**Figure 18. Damming Susceptibility Map of Formation of river stretches by new landslides in the lower Pskem basin. The black circle highlights a river stretch with unusually high values.** River network database from Coccia et al. (2023). Basemap source: Esri, HERE, Garmin Intermap, increment P Corp, GEBCO, USGS, FAO, NPS, NRCAN, GeoBase, IGN, Kadaster NL, Ordnance Survey, Esri Japan, METI, Esri China (Honk Kong), © OpenStreetMap contributors, and the GIS User Community.

## 4.2 The Fergana valley mountainous rim (Tajikistan-Kyrgyz Republic-Uzbekistan)

The Fergana valley is one of the largest intermountain depressions in Central Asia located between Uzbekistan, Kyrgyz Republic, and Tajikistan. It hosts two main rivers, the Naryn and the Kara Darya, which join together to form the Syr Darya. In this populated area landslide activity is recurrent, causing every year damage to infrastructure and loss of human life, and triggered by complex interactions between multiple factors such as tectonic, geological, morphological and meteorological (Danneels et al., 2008; Schlögel et al., 2011; Piroton et al., 2020). The mapping methodology have been applied also to the Fergana valley and a total of 3370 landslides, coming from various data sources, have been classified as shown in Figure 19. Comparably to the classification result of the entire inventory (Figure 9) most of the cases (94%) have a Very Low damming predisposition, followed by Low and Moderate (with 2.5% and 1.8% respectively) as reported in Table 4. Just very few landslides fall into High and Very High classes (with 1.4% and 0.3% respectively). For the classification of the river network of the Fergana valley, the maps of Damming Susceptibility of Non-formation and Formation have been produced (Figure 20 and Figure 21 respectively). As a method with a multi-scale approach, in such large areas, this damming

susceptibility method is suitable to provide territorial planning suggestions rather than indications on single interventions at local scale. The overall damming predisposition of the Fergana valley is quite low, considering the presence of 3370 mapped landslides in total, even if there are few landslides (10) classified with Very High damming predisposition which should be studied with more attention through localized analysis of damming susceptibility to ensure that downstream areas are not at risk and therefore require a specific monitoring.

Table 4 have been reported the distribution of the percentages of the damming susceptibility classes of those river stretches that are not running in flat areas, since these lowland rivers represent 53.6% of the total. Concerning the Damming Susceptibility Map of non-formation of the remaining river stretches (Figure 20), the most frequent are Low and Moderate classes with 53.4% and 36.2% respectively, followed by Very Low class with 7.0%. Only just 2.1% and 1.3% have been classified as Very High and High. For the Damming Susceptibility Map of Formation (Figure 21) most of the rivers fall into Very Low and Low classes with 54.5% and 38.1%, followed by Moderate class with 5.2%. Only 1.9% and 0.2% have been classified as Very High and High respectively.

**Table 4. Distribution of Damming Susceptibility classes on existing landslides (Figure 19) and on the river stretches for non-formation (Figure 20) and Formation of new landslides (Figure 21).**

| Damming Susceptibility | Landslides | | non-formation | Formation |
|---|---|---|---|---|
| | n. | % | % | % |
| Very High | 10 | 0.3% | 1.9 | 1.7 |
| High | 48 | 1.4% | 1.2 | 0.2 |
| Moderate | 61 | 1.8% | 7.0 | 5.3 |
| Low | 83 | 2.5% | 53.2 | 38.8 |
| Very Low | 3168 | 94.0% | 6.7 | 54.0 |

510
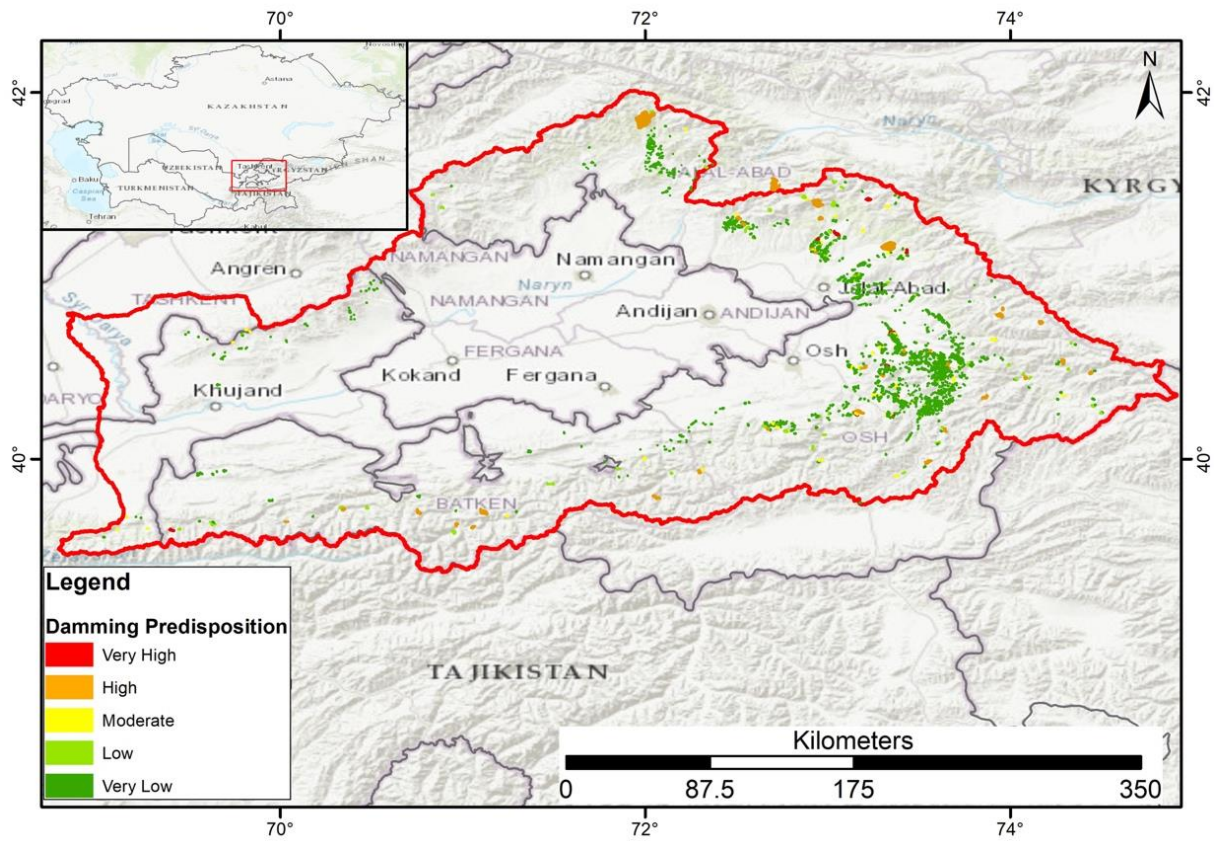
**Figure 19. Map of Damming Predisposition by landslides reactivation in the Fergana valley.** Basemap source: Esri, HERE, Garmin Intermap, increment P Corp, GEBCO, USGS, FAO, NPS, NRCAN, GeoBase, IGN, Kadaster NL, Ordnance Survey, Esri Japan, METI, Esri China (Honk Kong), © OpenStreetMap contributors, and the GIS User Community.

515
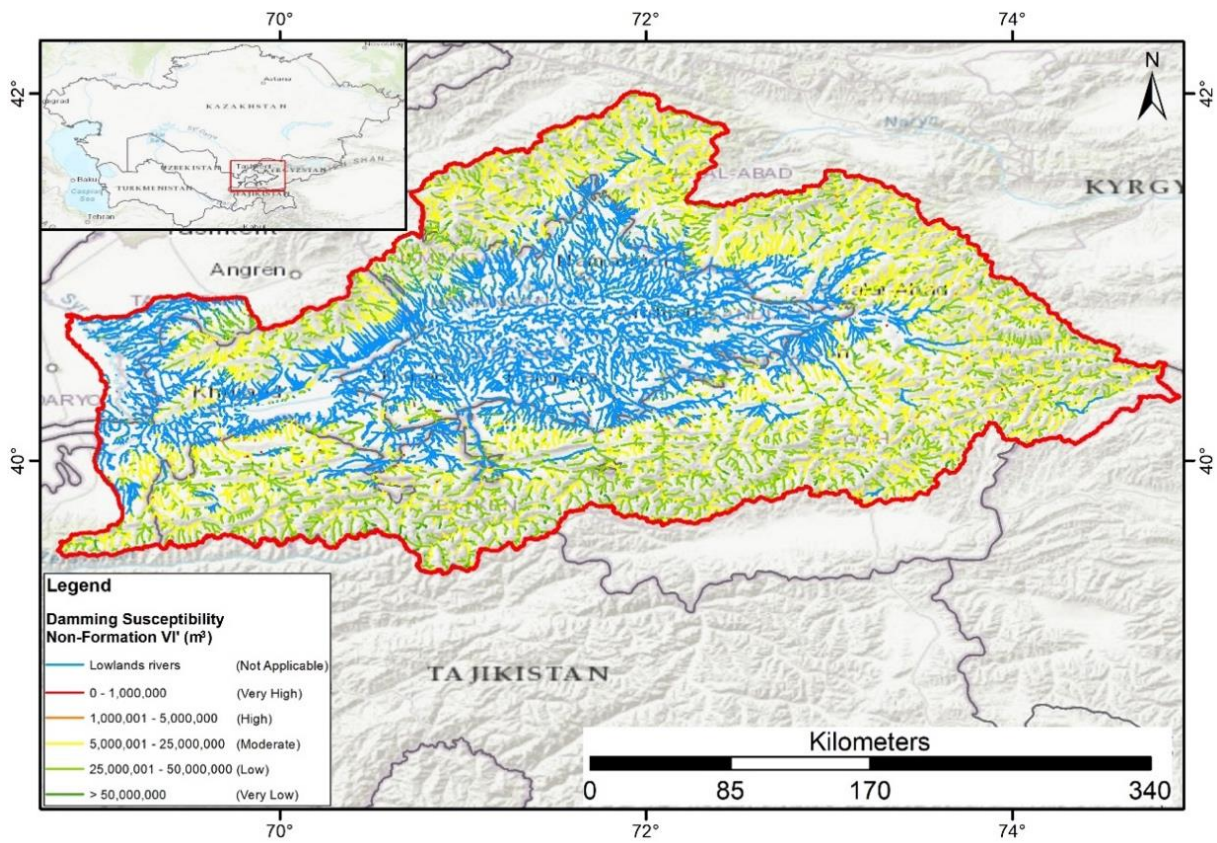
**Figure 20. Damming Susceptibility Map of Non-formation of river stretches by new landslides in the Fergana valley.** River network database from Coccia et al. (2023). Basemap source: Esri, HERE, Garmin Intermap, increment P Corp, GEBCO, USGS, FAO, NPS, NRCAN, GeoBase, IGN, Kadaster NL, Ordnance Survey, Esri Japan, METI, Esri China (Honk Kong), © OpenStreetMap contributors, and the GIS User Community.

521

**Figure 21. Damming Susceptibility Map of Formation of river stretches by new landslides in the Fergana valley.** River network database from Coccia et al. (2023). Basemap source: Esri, HERE, Garmin Intermap, increment P Corp, GEBCO, USGS, FAO, NPS, NRCAN, GeoBase, IGN, Kadaster NL, Ordnance Survey, Esri Japan, METI, Esri China (Honk Kong), © OpenStreetMap contributors, and the GIS User Community.

**5    Discussion**

During the application of the damming mapping methodology, the main issues encountered was the extremely wide study area, the amount of data and the processing time required. The used mapping methodology based on the MOI equations (Eq.(1)), was originally designed to assess the damming susceptibility at basin/regional scale (Tacconi Stefanelli et al., 2016; 2020), where the morphological parameters essential for the correct application of the tool proposed by Wood (2009) must be correctly found to have an accurate river width required in the MOI equations (Eq.(1)). This time-consuming phase has been simplified in this research, according to the wide dimension of the study area, taking into account not the basins but the different states in the Central Asia region. This simplification certainly affected the reliability of the individual specific data, while still guaranteeing an important overview of the general hazard distribution of the phenomenon in the area. Furthermore, the results quality is directly proportional to the resolution and quality of the input data, which on the other hand is inversely proportional to the processing time. In this regard, a further criticality of this process is the reliability on the landslides volumes assessment method, since a higher quality of landslides data (sliding geometry and depth) allows the application of a more accurate volume calculation and therefore a better final result.

Considering the size of the area, in Figure 9 the number of landslides classified with Very High damming predisposition (166 cases) is reasonable in absolute value, even if a bit high if compared with the total number of landslides present in the inventory (8910 cases). Without a detailed study it is not possible to say how many of these are false positives or not, however it is important to remember that this type of hazard mapping methods gives information on if and where, not when these events may occur. Although a validation of all the results is not possible, we can verify some of these through comparison with cases known in the, as shown in Figure 22. These landslides have been documented in Strom (2010) who has reported several landslide dams in Central Asia regions. In Table 5 their current conditions are compared with their Damming Predisposition classification using the methodology proposed here (before the intensity reduction of the classification by one class of those landslides that intersect the river network). From this information can be observe that 23 (77% of the total) of these landslides were correctly classified with the Very High predisposition value, 1 (3%) as High and 5 (17%) with Moderate. Only one landslide, No. 22 called Arashan in Strom (2010), was classified as Low predisposition despite it obstructed the Alamedin River and then collapsed and deeply eroded. This classification error can be explained by the missing landslide volume eroded by the river as a bigger value would probably have provided a higher predisposition. Based on this simple comparison, approximately 80% of the landslide dams analysed by Strom (2010) has a corrected Damming Predisposition value (Very High) based on their volume and the width of their valley. The final classification value of Damming Predisposition of all of them has been downgraded by one class as they intersect the river network (see Section 3 Materials and Methods).
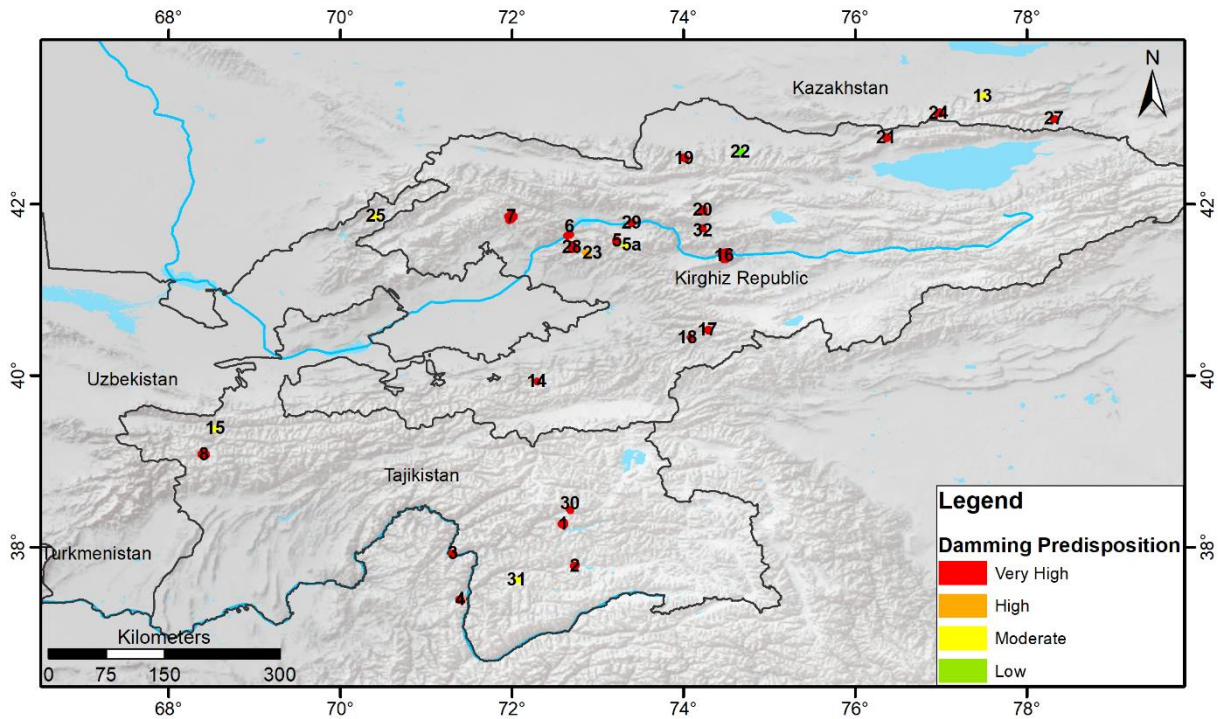
**Figure 22. Map of Damming Predisposition using landslide from Strom (2010).** See Table 5 for landslide numbers. Lake's polygons from Esri, Garmin International, Inc.; basemap from Esri, USGS, NOAA.

**Table 5. Information of landslides in Figure 22 (from Strom, 2010) and their Damming Predisposition**

**assessment.**

| N. | Name | Mountain chain-Region | Consequences | Damming Predisposition |
|---|---|---|---|---|
| 1 | Usoi | Pamirs-Tajikistan | Dammed (with lake) | Very High |
| 2 | Yashilkul | Pamirs-Tajikistan | Dammed (with lake) | Very High |
| 3 | Shids | Pamirs-Tajikistan | Dammed (with lake, partially breached) | Very High |
| 4 | Shiva | Pamirs-Afghanistan | Dammed (with lake) | Very High |
| 5 | Karasu | Tien Shan-Kyrgyz Rep. | Dammed (with lake) | Very High |
| 5a | Kapkatash | Tien Shan-Kyrgyz Rep. | Dammed (with lake) | Moderate |
| 6 | Karakul | Tien Shan-Kyrgyz Rep. | Dammed (filled lake) | Very High |
| 7 | Sarychelek | Tien Shan-Kyrgyz Rep. | Dammed (with lake) | Very High |
| 8 | Iskanderkul | Tien Shan-Tajikistan | Dammed (with lake) | Very High |
| 9 | Tianchi | Tien Shan-China | Dammed (with lake) | Very High |
| 11 | Twin-Lakes (upper) | Tien Shan-China | Dammed (with lake) | Very High |
| 12 | Twin-Lakes (lower) | Tien Shan-China | Dammed (with lake) | Very High |
| 13 | Issyk | Tien Shan-Kazakhstan | Dammed (with lake) | Moderate |
| 14 | Yashinkul | Tien Shan-Kyrgyz Rep. | Dammed (collapsed) | Very High |
| 15 | Aini | Tien Shan-Tajikistan | Dammed (lake artificially drained) | Moderate |
| 16 | Beshkiol | Tien Shan-Kyrgyz Rep. | Dammed (collapsed) | Very High |
| 17 | Kulun | Tien Shan-Kyrgyz Rep. | Dammed (with lake) | Very High |
| 18 | Kulun Mouth | Tien Shan-Kyrgyz Rep. | Dammed (filled lake) | Very High |
| 19 | Aksu | Tien Shan-Kyrgyz Rep. | Dammed (collapsed) | Very High |
| 20 | Kokomeren | Tien Shan-Kyrgyz Rep. | Dammed (collapsed) | Very High |
| 21 | Djashilkul | Tien Shan-Kyrgyz Rep. | Dammed (collapsed) | Very High |
| 22 | Arashan | Tien Shan-Kyrgyz Rep. | Dammed (collapsed) | Low |
| 23 | Kutmankul | Tien Shan-Kyrgyz Rep. | Dammed (with lake) | High |
| 24 | Bolshoe Almaty | Tien Shan-Kazakhstan | Dammed (with lake) | Very High |
| 25 | Badak | Tien Shan-Uzbekistan | Dammed (with lake) | Moderate |
| 28 | Dead Lakes | Tien Shan-Kyrgyz Rep. | Dammed (with lake) | Very High |
| 29 | Djuzumdybu-lak | Tien Shan-Kyrgyz Rep. | Dammed (with lake) | Very High |
| 30 | Kudara | Pamirs-Tajikistan | Dammed (collapsed) | Very High |

| 31 | Rivakkul | Pamirs-Tajikistan | Dammed (with lake) | Moderate |
|----|----------|-------------------|--------------------|----------|
| 32 | Ornok | Tien Shan-Kyrgyz Rep. | Dammed (collapsed) | Very High |

563

The two maps of damming susceptibility (Figure 11 and Figure 13), while not providing probability values as done by Tacconi Stefanelli et al. (2020), offer information (the volumes of landslides) that can be more easily spent and interpreted even by operators who are not specifically expert, and for this reason have more practical utility. Furthermore, the classification of the river stretches thus produced, not requiring the alpha parameter (linked to the probability of landslide occurrence) as in the original method proposed by Tacconi Stefanelli et al. (2020), it is much easier to obtain and for this reason it can be considered an improvement within a view of wider usability.

## 6    Conclusions

The price of a river obstruction, in terms of reconstruction and losses on both economic and lives, can be much higher compared with the costs of a proper environmental planning and land-use management. Be able to define the areas with higher risk could considerably lower the costs, allowing to focus the economic resources in effective preventive interventions, planning and monitoring activities.

In this work a damming mapping methodology have been proposed and carried out on the Central Asia regions as a part of a multi-hazard approach in the framework of the SFRARR Project ("Strengthening Financial Resilience and Accelerating Risk Reduction in Central Asia"). The used method, originally developed applying the Morphological Obstruction Index at basin scale, have been modified to fit such a large study area and the available data. Over 8000 landslides and the entire river network of studied area have been analyzed to propose a practical tool to assess where the damming susceptibility, from reactivation of mapped landslides and formation of new landslides, are higher at national scale. The improvement of the original method allows a simpler use on a wider area, as the technical knowledge and data required can also be managed by a non-expert operator, and the need for less data, more easily available. The main limitation of the work is related to the uncertainty of the reliability of the results at local scale due to the absence of a possible validation of all results, requiring many in-depth specific studies in the areas identified with the higher predisposition. This uncertainty can be improved in future studies by using data with better resolution, coverage, and quality.

Besides its limitations, this tool can be undoubted useful in very large countries where there is a lack of diffuse assessment of landslide activity, providing preliminary information about damming susceptibility to adopt risk reduction measures, for land management and as a starting point for future studies in specific areas potentially more subject to the damming hazard identified in this work.

*Code and data availability*. The landslide dam mapping susceptibility method was implemented by using the cited landslide inventory maps, published by the following authors: Behling et al., 2014, 2016, 2020; Havenith et al., 2015a; Strom and Abdrakhmatov, 2018. The SRTM DEM data are available from https://earthexplorer.usgs.gov/. The river network and other landslide inventories were provided by the SFRAAR project partners: RED (Risk, Engineering + Development – Pavia, Italy), OGS (National Institute of Oceanography and Experimental Geophysics, Seismological Research Center, Trieste, Italy), IWPHE (Institute of Water problems, Hydropower, Engineering and Ecology, Dushanbe, Republic of Tajikistan), ISASUZ (Institute of Seismology of the Academy

of Science of Uzbekistan, Tashkent, Uzbekistan), LLP (Institute of Seismology of the Science Committee of the Republic of Kazakhstan, Almaty).

*Author contribution.* Carlo Tacconi Stefanelli implemented the damming mapping method, William Frodella conceived with Carlo Tacconi Stefanelli the article structure and collected the data, Francesco Caleca supported the method application on part of the study area. Francesco Caleca also performed statistical analysis involving the method results. All the aforementioned Authors contributed to the writing of the article and the figure graphics. Veronica Tofani coordinated the work and reviewed the paper. Zhanar Raimbekova and Ruslan Umuraliev provided environment and geomorphology information and part of the landslide database for Kazakhstan and Kyrgyz Republic.

*Competing interests.* The contact author has declared that none of the authors has any competing interests.

*Acknowledgements.* This work was developed within World Bank-funded project "*Strengthening Financial Resilience and Accelerating Risk Reduction in Central Asia*" (SFRARR), in collaboration with the European Union, and the GFDRR (Global Facility for Disaster Reduction and Recovery), with the goal of improving financial resilience and risk-informed investment planning in the central Asian countries (Kazakhstan, Kyrgyz Republic, Tajikistan, Turkmenistan and Uzbekistan). This work brings the part of the results of the Task 7 "Landslide Scenario Assessment", managed by the UNESCO Chair on Prevention and Sustainable Management of Geo-Hydrological Hazards (University of Florence, Italy). In particular, the authors would like to thank Gabriele Coccia and Paola Ceresa from Red Risk Engineering (Pavia, Italy) for providing river network data and for the valuable coordination and constant support, and also Alexander Strom and Hans Balder Havenith for providing landslide inventories and for their constructive advice and valuable observations. We would also like to thank the partners from Central Asia for the fruitful collaboration, in particular: IWPHE (Tajikistan), ISASUZ and the State Monitoring Service of the Republic of Uzbekistan for tracking dangerous geological processes (Uzbekistan), the Institute of Seismology of the National Academy of Sciences of Kyrgyz Republic (ISNASKR), and the Institute of Seismology Limited Lability Partnership (LLP) of Kazakhstan.

*Financial support*. This research has been supported by the World Bank Group (Consulting Services Contract No. 8006611 – Regionally consistent risk assessment for earthquakes and floods and selective landslide scenario analysis for strengthening financial resilience and accelerating risk reduction in Central Asia).

**References**

Abdrakhmatov, K.Y., Aldazhanov, S.A., Hager, B.H., Hamburger, M.W., Herring, T.A., Kalabaev, K.B., Makarov, P., Molnar, S.V., Panasyuk, M.T., Prilepin, R.E., Reilinger, I.S., Sadybakasov, B.J., Souter, Yu.A., Trapeznikov, V.Ye., and Tsurkov Zubovich, A.V.: Relatively recent construction of the Tien Shan inferred from GPS measurements of present-day crustal deformation rates. Nature, 384(6608), 450-45319, 1996.

Abdrakhmatov, K., Havenith, H.B., Delvaux, D., Jongmans, D., and Trefois, P.: Probabilistic PGA and Arias Intensity Maps of Kyrgyz Republic (Central Asia). J. Seismol. 7.2: 203-220, 2003.

Behling, R., Roessner, S., Kaufmann, H., and Kleinschmit, B.: Automated spatiotemporal landslide mapping over large areas using rapideye time series data. Remote Sens. 6, 8026–8055, 2014.

Behling, R., Roessner, S., Golovko, D., and Kleinschmit, B.: Derivation of long-term spatiotemporal landslide activity—A multi-sensor time series approach. Remote Sens. Environ. 186, 88–104, 2016.

Behling, R., and Roessner, S.: Multi-temporal landslide inventory for a study area in Southern Kyrgyz Republic derived from RapidEye satellite time series data (2009 – 2013). V. 1.0. GFZ Data Services. https://doi.org/10.5880/GFZ.1.4.2020.001, 2020.

Borgatti, L., and Soldati, M.: Landslides as a geomorphological proxy for climate change: a record from the Dolomites (northern Italy), Geomorphology, 120(1–2), 56–64, 2010.

CAC DRMI: Risk assessment for Central Asia and Caucasus: desk study review, 2009.

Canuti, P., Casagli, N., Ermini, L., Fanti, R., and Farina, P.: Landslide activity as a geoindicator in Italy: significance and new perspectives from remote sensing, Environ. Geol., 45(7), 907–919, 2004.

Casagli, N., and Ermini, L.: Geomorphic analysis of landslide dams in the Northern Apennine, Trans. Jpn. Geomorphol. Union., 20(3), 219–249, 1999.

Catani, F., Tofani, V., and Lagomarsino, D.: Spatial patterns of landslide dimension: a tool for magnitude mapping, Geomorphology 273, 361–373. https://doi.org/10.1016/j.geomorph.2016.08.032, 2016.

Chedia, O.K., and Lemzin, I.N.: Seismogenerating faults of the Chatkal depression. In: Seismotectonics and seismicity of the Tien Shan. Frunze, Ilim, 18–28, 1980.

Chen, C.Y., Chang, J.M.: Landslide dam formation susceptibility analysis based on geomorphic features. Landslides, 13(5), 1019-1033, 2016.

Coccia, G., Ceresa, P., Bussi, G., Denaro, S., Bazzurro, P., Martina, M., Fagà, E., Avelar, C., Ordaz, M., Huerta, B., Garay, O., Raimbekova, Z., Abdrakhmatov, K., Mirzokhonova, S., Ismailov, V., and Belikov, V.: Large-scale flood risk assessment in data scarce areas: an application to Central Asia, Nat. Hazards Earth Syst. Sci. Discuss. [preprint], https://doi.org/10.5194/nhess-2023-157, under review, 2023.

Costa, J.E., and Schuster, R.L.: Documented historical landslide dams from around the world. US Geol. Surv. Open-File Report, 91(239), 1-486, 1991.

Costa, J.E., and Schuster, R.L.: Formation and failure of natural dams. Bull Geol Soc Am, 1 0 0 (7), 1054–1068. https://doi.org/10.0016-1988)100/0016-7606(1988)100<1054:TFAFON>2.3.CO, 1988.

Crozier, M.J.: Deciphering the effect of climate change on landslide activity: a review, Geomorphology, 124(3), 260–267, 2010.

Dai, F.C., Lee, C.F., Deng, J.H., Tham, L.G.: The 1786 earthquake-triggered landslide dam and subsequent dam-break flood on the Dadu River, southwestern China. Geomorphology, 65(3), 205-221, 2005.

Dal Sasso, S.F., Sole, A., Pascale, S., Sdao, F., Bateman Pinzòn, A., and Medina, V.: Assessment methodology for the prediction of landslide dam hazard, Nat. Hazards Earth Syst. Sci., 14 (3), 557–567, http://dx.doi.org/10.5194/nhess-14-557-2014, 2014.

667 Danneels, G., Bourdeau, C., Torgoev, I., Havenith, H.B.: Geophysical investigation and dynamic modelling of
668     unstable slopes: case-study of Kainama (Kyrgyzstan). Geophys. J. Int., 175(1), 17-34, 2008.

669 Delvaux, D., Abdrakhmatov, K.E., Lemzin, I.N., and Strom, A.L.: Landslides and surface breaks of the 1911 Ms
670     8.2 Kemin earthquake, Kyrgyzstan, Russian Geology and Geophysics, 2001, 42, 10, 1667-1677, 2001.

671 Dikau, R., and Schrott, L.: The temporal stability and activity of landslides in Europe with respect to climatic
672     change (TESLEC): main objectives and results, Geomorphology, 30(1–2), 1–12, 1999.

673 Drăguţ, L., and Dornik, A.: Land-surface segmentation as a method to create strata for spatial sampling and its
674     potential for digital soil mapping, Int. J. Geogr. Inf. Sci., 30(7), 1359-1376, 2016.

675 Ermini, L., Casagli, N.: Prediction of the behavior of landslide dams using a geomorphical dimensionless index,
676     Earth Surf Proc Land 28:31–47. https://doi.org/10.1002/esp.424, 2003.

677 Falátková, K.: Temporal analysis of GLOFs in high-mountain regions of Asia and assessment of their causes,
678     AUC Geographica, 51, 2, 145–154, 2016.

679 Fan, X., Rossiter, D.G., van Westen, C.J., Xu, Q., and Görüm, T.: Empirical prediction of coseismic landslide dam
680     formation, Earth. Surf. Proc. Land., 39(14), 1913–1926, 2014.

681 Fan, X., Dufresne, A., Subramanian, S.S., Strom, A., Hermanns, R., Tacconi Stefanelli, C., Hewitt, K., Yunus,
682     A.P., Dunning, S., Capra, L., Geertsema, M., Miller, B., Casagli, N., Jansen, J.D., and Xu, Q.: The formation
683     and impact of landslide dams – State of the art, Earth Sci. Rev., 203, 103116,
684     https://doi.org/10.1016/j.earscirev.2020.103116, 2020.

685 Fan, X., Dufresne, A., Whiteley, J., Yunus, A.P., Subramanian, S.S., Okeke, C.A., Pánek, T., Hermanns, R., Ming,
686     P., Strom, A., Havenith, H.B., Dunning, S., Wang, G., and Tacconi Stefanelli, C.: Recent technological and
687     methodological advances for the investigation of landslide dams, Earth-Sci. Rev., 218, 103646,
688     https://doi.org/10.1016/j.earscirev.2021.103646, 2021.

689 Farr, T.G., and Kobrick, M.: Shuttle Radar Topography Mission produces a wealth of data. Eos Trans. AGU, 81,
690     583-583, 2000.

691 Golovko, D., Roessner, S., Behling, R., Wetzel, H.U., and Kleinschmidt, B.: Development of multi-temporal
692     landslide inventory information system for southern Kyrgyz Republic using GIS and satellite remote sensing,
693     PFG, 2015(2), 157–172, 2015.

694 Guzzetti, F., Ardizzone, F., Cardinali, M., Rossi, M., and Valigi, D.: Landslide volumes and landslide mobilization
695     rates in Umbria, central Italy, EPSL, 279, 222–229, 2009.

696 Havenith, H.B., Strom, A., Cacerez, F., and Pirard, E.: Analysis of landslide susceptibility in the Suusamyr region,
697     Tien Shan: statistical and geotechnical approach. Landslides 3, 39–50, 2006a.

698 Havenith, H.B., Torgoev, I., Meleshko, A., Alioshin, Y., Torgoev, A., and Danneels, G.: Landslides in the Mailuu-
699     Suu Valley, Kyrgyz Republic—hazards and impacts, Landslides, 3, 137–147, 2006b.

Havenith, H.B., Strom, A., Torgoev, I., Torgoev, A., Lamair, L., Ischuk, A., and Abdrakhmatov, K.: Tien Shan geohazards database: Earthquakes and landslides, Geomorphology, 249, 16–31, 2015a.

Havenith, H.B., Torgoev, A., Schlögel, R., Braun, A., Torgoev, I., and Ischuk, A.: Tien Shan geohazards database: Landslide susceptibility analysis, Geomorphology, 249, 32–43, 2015b.

Havenith, H.B., Umaraliev, R., Schlögel, R., Torgoev, I., Ruslan, U., Schlogel, R., and Torgoev, I.: Past and Potential Future Socioeconomic Impacts of Environmental Hazards in Kyrgyz Republic. In Kyrgyz Republic: Political, Economic and Social Issues; Olivier, A.P., Ed.; Nova Science Publishers, Inc.: Hauppauge, NY, USA; pp. 63–113, 2017.

Hungr, O., and Evans, S.G.: Entrainment of debris in rock avalanches: an analysis of a long run-out mechanism, Geol. Soc. Am. Bull., 116(9-10), 1240-1252, 2004.

Juliev, M., Pulatov, A., and Hubl, J.: Natural hazards in mountain regions of Uzbekistan: A review of mass movement processes in Tashkent province. International Journal of Scientific and Engineering Research, 8(2), 1102, 2017.

Kalmetieva, Z.A., Mikolaichuk, A.V, Moldobekov, B.D., Meleshko, A.V, Janaev, M.M., and Zubovich, A.V.: Atlas of earthquakes in Kyrgyz Republic. Central-Asian Institute for Applied Geosciences and United Nations International Strategy for Disaster Reduction Secretariat Office in Central Asia, Bishkek, p 75, 2009.

King, J., Loveday, I., Schuster, R.L.: The 1985 Bairaman landslide dam and resulting debris flow, Papua New Guinea. Q J Eng Geol Hydroge, 22(4), 257-270, 1989.

Kropáček, J., Vilímek, V., and Mehrishi, P.: A preliminary assessment of the Chamoli rock and ice avalanche in the Indian Himalayas by remote sensing, Landslides, 18, 3489–3497, https://doi.org/10.1007/s10346-021-01742-1, 2021.

Liao, H.M., Yang, X.G., Lu, G.D., Tao, J., and Zhou, J.W.: A geotechnical index for landslide dam stability assessment, Geomatics, Natural Hazards and Risk, 13(1), 854-876, https://doi.org/10.1080/19475705.2022.2048906, 2022.

Maxwell, A.E., and Shobe, C.M.: Land-surface parameters for spatial predictive mapping and modeling, Earth-Sci. Rev., 226, 103944, 2022.

Molnar, P., and Tapponnier, P.: Cenozoic Tectonics of Asia: Effects of a Continental Collision: Features of recent continental tectonics in Asia can be interpreted as results of the India-Eurasia collision. science, 189(4201), 419-426, 1975.

Niyazov, R.A.: Uzbekistan landslides. Uzbekistan landslide service. Technical report, 2020.

Peresan, A., Scaini, C., Tyagunov, S., and Ceresa, P.: Capacity Building Experience for Disaster Risk Reduction in Central Asia, Nat. Hazards Earth Syst. Sci. Discuss. [preprint], https://doi.org/10.5194/nhess-2023-156, in review, 2023.

Persits, F.M., Ulmishek, G. F., Steinshouer, D.W.: Maps showing geology, oil and gas fields and geologic

provinces of the Former Soviet Union (No. 97-470-E). US Geological Survey, https://doi.org/10.3133/ofr97470E, 1997.

Petrov, M.A., Sabitov, T.Y., Tomashevskaya, I.G., Glazirin, G.E., Chernomorets, S.S., Savernyuk, E.A., Tutubalina O.V., Petrakov, D.A., Sokolov, L.S., Dokukin, M.D., Mountrakis, G., Ruiz-Villanueva, V., and Stoffel, M.: Glacial lake inventory and lake outburst potential in Uzbekistan, Sci. Total Environ., 592, 228-242, 2017.

Piroton, V., Schlögel, R., Barbier, C., and Havenith, H.B.: Monitoring the recent activity of landslides in the Mailuu-suu valley (Kyrgyz Republic) using radar and optical remote sensing techniques. Geosciences, 10 (5), p. 164, 2020.

Popescu, M.E., and Sasahara, K.: Engineering Measures for Landslide Disaster Mitigation, in: Landslides – Disaster Risk Reduction, edited by: Sassa, K., Canuti, P., Springer, Berlin, Heidelberg, 609-631, https://doi.org/10.1007/978-3-540-69970-5_32, 2009.

Righini, M., and Surian, N.: Remote sensing as a tool for analysing channel dynamics and geomorphic effects of floods, Flood monitoring through remote sensing, 27-59, 2018.

Rosi, A., Frodella, W., Nocentini, N., Caleca, F., Havenith, H.B., Strom, A., Saidov, M., Bimurzaev, G.A., and Tofani, V.: Comprehensive landslide susceptibility map of Central Asia, Nat. Hazards Earth Syst. Sci., 23, 2229–2250, https://doi.org/10.5194/nhess-23-2229-2023, 2023.

Saponaro, A., Pilz, M., Wieland, M., Bindi, D., Moldobekov, B., and Parolai, S.: Landslide susceptibility analysis in data-scarce regions: the case of Kyrgyz Republic. Bull. Eng. Geol. Environ. 74, 1117–1136, 2014.

Schlögel, R., Torgoev, I., De, Marneffe, C., and Havenith, H.B.: Evidence of a changing size-frequency distribution of landslides in the Kyrgyz Tien Shan, Central Asia. Earth Surf Process Landf 36(12), 1658–1669, 2011.

Schuster, R.L., and Evans, S.G.: Engineering Measures for the Hazard Reduction of Landslide Dams, in: Natural and Artificial Rockslide Dams. Lecture Notes in Earth Sciences, edited by: Evans, S., Hermanns, R., Strom, A., Scarascia-Mugnozza, G., Springer, Berlin, Heidelberg, https://doi.org/10.1007/978-3-642-04764-0_2, 2011.

Semakova, E., Gunasekara, K., and Semakov, D.: Identification of the glaciers and mountain naturally dammed lakes in the Pskem, the Kashkadarya and the Surhandarya River basins, Uzbekistan, using ALOS satellite data, Geomat. Nat. Hazards Risk, 7(3), 1081-1098, 2016.

Styron, R., Pagani, M.: The GEM Global Active Faults Database." Earthquake Spectra, vol. 36, no. 1_suppl, Oct. 2020, pp. 160–180, https://doi.org/10.1177/8755293020944182, 2020.

Strom, A.: Landslide dams in Central Asia region. Journal of the Japan Landslide Society, 47(6), 309-324, 2010.

Strom, A., and Abdrakhmatov, K.: Large-Scale Rockslide Inventories: From the Kokomeren River Basin to the Entire Central Asia Region (WCoE 2014–2017, IPL-106-2, in: Workshop on World Landslide Forum. Springer, Cham, pp. 339–346, 2017.

769  Strom, A., and Abdrakhmatov. K.: Rockslides and rock avalanches of Central Asia: distribution, morphology, and
770      internal structure. Elsevier, 441pg. ISBN: 978-0-12-803204-6, 2018.

771  Swanson, F.J., Oyagi, N., and Tominaga, M.: Landslide dams in Japan, in: Landslide dams: processes, risk and
772      mitigation, vol 3, edited by: Schuster R.L., Geotech. Sp., ASCE, New York, 131–145, 1986.

773  Tacconi Stefanelli, C., Catani, F., Casagli, N.: Geomorphological investigations on landslide dams. Geoenv Disast
774      2(1):1–15. https://doi.org/10.1186/s40677-015-0030-9, 2015.

775  Tacconi Stefanelli, C., Segoni, S., Casagli, N., and Catani, F.: Geomorphic indexing of landslide dams evolution,
776      Eng. Geol., 208, 1–10. https://doi.org/10.1016/j.enggeo.2016.04.024, 2016.

777  Tacconi Stefanelli, C., Vilímek, V., Emmer, A., and Catani, F.: Morphological analysis and features of the
778      landslide dams in the Cordillera Blanca, Peru, Landslides, 15(3), 507-521, https://doi.org/10.1007/s10346-
779      017-0909-5, 2018.

780  Tacconi Stefanelli, C., Casagli, N., and Catani, F.: Landslide damming hazard susceptibility maps: a new GIS-
781      based procedure for risk management, Landslides, 17, 1635-1648, https://doi.org/10.1007/s10346-020-
782      01395-6, 2020.

783  Trifonov, V.G., Makarov, V.I., and Scobelev, S.F.: The Talas-Fergana active right-slip faults. Ann Tectonicae
784      6:224–237, 1992.

785  Ullah, S., Bindi, D., Pilz, M., Danciu, L., Weatherill, G., Zuccolo, E., Anatoly Ischuk, A., Mikhailova, N.N.,
786      Abdrakhmatov, K., and Parolai, S.: Probabilistic seismic hazard assessment for Central Asia. Annals of
787      Geophysics, 58(1), 2015.

788  Wang, X., Ding, Y., Liu, S., Jiang, L., Wu, K., Jiang, Z., and Guo, W.: Changes of glacial lakes and implications
789      in Tian Shan, central Asia, based on remote sensing data from 1990 to 2010, Environ. Res. Lett., 8(4),
790      044052, 2013.

791  Wang, D., Laffan, S.W., Liu, and Y., and Wu, L.: Morphometric characterization of landform from DEMs, Int. J.
792      Geogr. Inf. Sci., 24(2), 305–326, 2010.

793  Wood, J.: Geomorphometry in LandSerf. In: Hengl, T. and Reuter, H.I. [Eds.]: Geomorphometry: Concepts,
794      Software, Applications, Dev. Soil. Sci., 33, 333-349, 2009.

795  Zubovich, A.V., Wang, X.Q., Scherba, Y.G., Schelochkov, G.G., Reilinger, R., Reigber, C., Mosienko, O.,
796      Molnar, P., Michajljow, W., Makarov, V.I., Li, J., Kuzikov, S.I., Herring, T.A., Hamburger, M.W., Hager
797      B.H., Dang, Y., Bragin, V.D., and Beisenbaev, R.: GPS velocity field for the Tien Shan and surrounding
798      regions. Tectonics, 29(6), 2010.